Dear editor,

Thank you for considering our article for publication in SOIL. The two anonymous reviews were very useful for improving our manuscript. Below we provided our response, page and line numbers refer to the final manuscript. Next to the reviews, we also improved the uplift curve, as suggested by Eric Brevik in Short Comment C685 on the interactive discussion site of the paper. This consequently affected the calculated process rates and model results, which are therefore updated in this version. However, the changes were not so substantial as to affect the interpretations and conclusions.

Response to reviewer 1.

We would like to thank reviewer 1 for his/her time and effort to review our article on Arctic soil development. The comments provided are very useful and will certainly improve the article. Here we respond to the comments.

Major concerns

1) Ages of the terraces The presentation of the age constraints is quite confusing. Surface ages are reported to a certain extent already in the text, in chapter 2.1. Some references are given and the reader is referred to Fig. 1. The authors report about the 6 terraces but no real ages are shown (for the individual terraces). A correlation of ages with altitude is shown in Fig. 3, but much later on – but no relation to the terraces is given. So, the reader is fed portion-wise with surface age data – and this makes the lecture of the manuscript quite difficult. I furthermore did not find out the ages of all terraces (even after having read the whole manuscript). Please create an additional table where each terrace is assigned to a specific age or age range.

RESPONSE: In the revised manuscript we paid more attention to the existing ages of the different terrace levels, in order to make it a more coherent story (P. 6, lines 136-142, Figs 1 and 3). We did not date all major terrace levels, but the combination of our OSL dates with earlier radiocarbon dates cover most of them. Please note that the major terrace levels contain smaller ridge and valley sequences, thus several ages. With the relation between altitude and age we have derived the age constraints of each major terrace level, but this is one of the results of the study, just like the OSL ages, and is thus reported in the Results section (in Table 3, as the reviewer suggests).

2) Soil data: The soil dataset should be presented in a better legible way. What is the use of Table 3? It only shows the average (±SD) of the entire dataset of some soil parameters. Why not presenting this dataset for each terrace? The reader would then have the possibility to see how these parameters are changing as a function of time. Or include at least the parameters such as the CaCO3 content, BD and horizon thickness in Figure 5 and give an earlier reference to this figure in the text (I however would prefer a table). Furthermore, Fig. 5 suggests that all soils have the same horizons. Is this really true?

RESPONSE: With Table 3 we aimed to show summary statistics of the observed soil properties for the study area. We have now extended the table and present soil properties per horizon per terrace level. Fig. 5 acts as a visualization of Table 3. In our opinion, this visualization is helpful in better understanding possible trends in the soil properties. We have extended this Figure with bulk density and horizon thickness for a more complete picture. We have also added the number of occurrences for each box in Fig. 5, to show that not every horizon is found in each soil.

In addition, the horizon designation is slightly confusing. Here maybe some more explanations could be given in the methods section) I know which principle has been employed (it is explained in the text). E.g. Fig. 4: The 'typical' soil left seems to have an aeolian deposit on top (this seems to be the C-material, right?). If 1 now stands for aeolian material and 2 for marine material, should the horizon sequence not be the following: 1C, 1bA, 2bA, 2bB . . .? In addition, the horizon 'B/' appears (which was obviously proposed by Forman and Miller, 1984). This seems to be a designation that neither exists in the WRB nor in the Soil Taxonomy. It seems to stand for 'silt illuviation'. But when having a look at Fig. 5, I do not see a higher silt concentration in the B/ horizon. (furthermore, part of the figure is cut off . . . silt fraction of T3). What are the process for silt illuviation?

RESPONSE: We did not adapt the formal WRB horizon designation, because it is easier to compare similar horizons when they are given the same name. Therefore we named all marine horizons 2A, 2B, 2B*l* or 2BC, although indeed only some of them are buried below the aeolian deposits. We have explained this better in the text, where we also mention the correct horizon designations (P.10-11, lines 248-267). Organic matter can be found throughout the sandy aeolian cover. Therefore we previously named it an A horizon. However, you have convinced us that the designation 1AC is more appropriate, and we have used it in the revised paper. Evidence for silt eluviation are the increase of silt concentration of B*l* horizons with age, while the concentration in 2A horizons decreases (Fig. 5). Next to that, the belly shaped curves in Fig. 7 also show an enrichment of silt in the subsurface. The very porous gravelly soils enable percolation of water, which can transport silt. In the field we could see evidence of this process by layers of silt on top of rocks and soil layers where the matrix was enriched with silt (B*l* horizons) (P. 18, lines 4342-445). The small case italic L (*l*) indicates the pedogenic accumulation of silt. We have better explained the processes behind silt eluviation in the manuscript (P. 7, lines 164-171).

3) more details about OSL dating: How were the samples taken? Were really marine samples analysed? Why should such a material be suitable for dating? How should bleaching have occurred? . . . Or did you sample the loess deposits? This needs to be better explained.

RESPONSE: Thank you for pointing out that details about the OSL dating were missing. We have now elaborated on the OSL dating in the Methods section (P. 9, lines 193-202).

Minor points

p. 1347, L. 25: what is 'relative' physical weathering?

RESPONSE: This referred to the relative contribution of physical and chemical weathering. We have rephrased this.

p. 1349, L. 9-23: if terraces are so complicated – why did you choose them for your investigation?

RESPONSE: We chose marine terraces because they exhibit a chronosequence of long-term Arctic soil development. The mentioned complicating factors distort the temporal signal, but they give valuable information on spatial drivers of soil formation. Therefore the marine terraces are suitable for the study of long term Arctic soil development on a landscape scale. We elaborated on this in the manuscript (P 4, lines 78-79, 100-101).

p. 1350, L. 6-17: should maybe be moved to the methods section.

RESPONSE: We used this paragraph to introduce the structure of the paper, like a reading guide. In the Methods section we elaborate on all mentioned methods. Therefore we believe it is suited for the Introduction.

p. 1351, L. 19-22: this sentence is not understandable.

RESPONSE: We have removed this sentence and elaborated more on the results of Long et al. (2012), as mentioned earlier in this response.

p. 1355, L. 18: '. . .. horizons were not cryic'. This is difficult to believe for such an environment. Please explain. p. 1361, L. 20-21: Phaeozems and Chernozems. Sure? They would testify quite a different climate that obviously had existed in the past. p. 1361, L. 17-24: Several soil units are mentioned here but the reader cannot allocate them to the terraces. As mentioned already above, the soil data should be better presented. Instead of Fig. 5 a table showing all parameters (see above) per terrace unit (average values ± SD) and soil units should be presented.

RESPONSE: we omitted the fact that all soils were probably Cryosols, in order to better describe the variation in observed soils. However, as this leads to confusion, e.g. on the genesis of the soils, we have now used the proper WRB classification and used qualifiers to indicate the observed soil diversity (P. 17-18, lines 425-435). The variation in soil units mainly depends on morphological setting instead of age, as is mentioned in the text. This is in fact a main result of the paper. Therefore it would not be useful to include the soil units in Table 3, which shows temporal variation. We now better describe how the different soils are positioned in the landscape.

p. 1356, L. 5: ANOVA → do you have a normal distribution of the datasets?

RESPONSE: The residuals of a linear model with soil properties and terrace level, soil horizon and morphological position were normally distributed (P 11-12, lines 278-283). Therefore the use of ANOVA was justified. For the silt fraction, we had to apply a log transformation to achieve normality. This is now updated in the new version.

p., L. 19: why a log function? Published data that substantiate such an assumption?

RESPONSE: The physical weathering equation in LORICA results in an exponential decay of coarse material. Therefore we used this formulation to calculate the weathering rate. Fig. 5 also suggests an exponential decay of gravel fraction for the 2B*l* and 2BC horizon. We have explained this better in the revision (P 15, lines 377-379).

p. 1361, L. 12: ' . . .approximately 14393 years old' . . .. I think you know what I mean . . .

RESPONSE: That age is indeed not very approximate. As this age serves as input for the model, we left out the ‘approximate’ and only noted the age (13300 years, following from the new uplift curve). (P 17, line 418-419).

p. 1362, L. 20: R2 = 0.29: is this significant? p. 1367, L. 6-7: where is this regression presented?

RESPONSE: The p-value of this regression is 0.007, and can therefore be considered significant (P. 19, lines 463-464).This is the same regression as referred to later in the text (second comment). We clarified this in this section (P. 24, lines 600-601).

p. 1362, L. 23: where is this number coming from? How was it determined? (please show it in a way that it is traceable for the reader).

RESPONSE: This number follows from Eq. 4 and the procedure explained on page 1359, L. 22-25. We have explained this now better in the main text (P. 19, line 4567)

p. 1366, L. 11-15: what about permafrost? I assume that there is permafrost. How deep is the active layer?

RESPONSE: With the impermeable layer mentioned in Section 5.2 we indeed mean permafrost table (and to a lesser extent the active layer). We have now clarified this (P. 23, line 579-580). The thickness of the active layer in the vicinity of the study area varies between 0.3 and 2.5 m (Gibas et al., 2005), with thaw depths on the marine terraces ranging from 0.45 to 1.20 m below the surface (Rachlewicz and Szczuciński, 2008) (added to P. 7, lines 158-160).

p. 1367, L. 2: two times ‘from the simulated’

RESPONSE: One time removed.

p. 1367, L. 28: Fig. 7 does not show a spatial distribution.

REPSONSE: Changed to: “This expected variation in weathering between different morphological settings was observed in particle size distributions (Fig. 7),…” (P. 24, lines 621-622).

p. 1368, L. 4: physical weathering? (if calculated from the gravel fraction. . .).

RESPONSE: Correct, we have changed it.

Technical corrections: Table 3 (in my opinion not that useful). But if used, please use more common units for BD, such as t/m3, kg/dm3 or g/cm3

RESPONSE: We have adapted to g/cm^3.

Response to reviewer 2

We thank reviewer 2 for the time put into reading and reviewing our manuscript. Below we provide our response.

General remarks The paper should be revised by an English speaking person. Some key phrases during the paper should be more supported by references.

RESPONSE: We have let an experienced native English speaker review the level of English in the final manuscript.

Abstract The abstract is a little confused and also a bit long.

RESPONSE: We have reformulated and shortened the abstract.

Introduction Page 1348 Line 20: Difference of the properties of the soils is not only attributed to age. Please rephrase. Line 20 to 23: Support this part with a reference.

RESPONSE: Nuances to this sentence are made in the next sentence, where we discuss that variation in other soil forming factors is equal for all soils in the study area. We have rephrased these sentences to: "In chronosequences, the only soil forming factor that is significantly different for all soils is time. Variation in the other soil forming factors, i.e. landscape position, climate, lithology and organisms, is assumed equal for all soils in the study area. Consequently, variation in soil properties can be mainly attributed to the age of the soils (Vreeken, 1975)." (P. 3, lines 63-66)

Page 1349 Line 5 to 20: Support this part with more references.

RESPONSE: We have included more references on the use of marine terraces as chronosequences.

Page 1356 Line 15: Refer to the method used for grain size classes.

RESPONSE: The method for determining grain size classes is dry sieving, as is mentioned on Page 1355, L. 26-27. (P. 11, lines 274-276 of revised manuscript).

Line 20 to 22: Please rephrase.

RESPONSE: Rephrased to: "Geomorphic processes are oriented laterally and only affect the top soil layer. Pedogenic processes are oriented vertically and alter material or transport material from one soil layer to another." (P. 12, lines 298-300)

Page 1360 Line 15: Why only use one of the processes?

RESPONSE: Here we intended to say that only one process is calibrated using the data. However, the same data were used to validate the model results. The model results are the result of several processes. Therefore the calibrated parameter does not correspond 1 to 1 on the model results. As this is a logical consequence of modelling and because the meaning of the sentence was unclear, we have removed this sentence.

Page 1364 Line 21 to 24: Please rephrase.

RESPONSE: Rephrased to: "The fitted uplift curve suggests that the youngest terrace is around 1500 years old. That could indicate that uplift has stagnated or reversed, leading to flooding of lower lying terraces, as is also suggested by Long et al. (2012) and (Strzelecki, 2012). This corresponds to renewed glacier growth in response to a cooler climate starting 3000 years ago, which eventually led to the Little Ice Age (Rachlewicz et al., 2013; Svendsen and Mangerud, 1997a)." (P. 21, lines 549-543)

Page 1365 Line 3 to 9: This part need a better explanation and support with references.

RESPONSE: We have better explained the methodological comparison between OSL and radiocarbon dating and supported it with references.

Page 1368 Line 6 to 11: This part need a better explanation and support with references.

RESPONSE: We have now elaborated on the effects of dissolution on the particle size distribution of the soil.

Page 1367 and 1368 (5.3 Soil Formation): SEM analysis would have been very useful for this paper, especially for the understanding of the weathering rates. Also, detailed profiles of the marine terraces, organic matter and silt content would also serve as a good support.

RESPONSE: We agree with the reviewer that SEM analysis would have been a valuable contribution for better understanding the weathering rates. However, as this research is an exploratory study on soil formation on a landscape scale, detailed analyses such as SEM and more detailed profile descriptions were beyond the scope of this study. We mentioned these methods in the Discussion, as a consideration for future studies (P. 24-25, lines 634-636 and P. 27, lines 703-704).

Page 1370 (5.4) To better explain the temporal interaction, a Table comparing your dates and from surrounding areas would support your results.

RESPONSE: We thank the reviewer for this suggestion, but comparing absolute ages from our study with those for surrounding areas may not produce useful information if they are not placed into context. It can also prove difficult for methodological reasons, because older radiocarbon dates are often not calibrated or corrected for the marine reservoir effect and therefore not directly comparable to OSL dates. A comparison of our uplift curve with other curves is more meaningful. We used our datings for reconstructing an uplift-curve. This was compared with surrounding uplift curves (P. 21, lines 517-538). As suggested by Eric Brevik (Short Comment 685 on interactive discussion of this paper), we constructed a new uplift curve, which better matches curves found in studies done in surrounding areas.

Conclusion Page 1371, line 25-page 1372, line 1 to 3: It is not clear the signs of the physical and chemical weathering. A quartz grain analyses using SEM would support this conclusion.

RESPONSE: The signs of physical weathering refer to a decrease in the coarse fraction. Evidence of chemical weathering was derived from the presence of secondary carbonates on rocks in the soil. Together these processes affect the complete particle size distribution of the soil. SEM might indeed have supported this conclusion, but as mentioned earlier, this was outside the scope of this study. We rephrased this conclusion to: "The changes in soil properties of the gravelly soils on the marine terraces can be attributed to different soil forming processes, such as physical (frost action) and chemical weathering (dissolution) and translocation of silt. Dissolution mainly occurs in A horizons developed in marine material. Translocation of silt occurs everywhere in the landscape, following the water flow." (P. 29, lines 738-742)

Page 1372 Lines 4 to 7: OSL is a good dating technique, but you only have 3 dates that could not be enough. You should compare your dates, with others from nearby areas.

RESPONSE: Our three dates support earlier radiocarbon datings on the same terraces. We agree with the reviewer that 3 dates are not sufficient to draw hard conclusions, and therefore we weakened the conclusion to: “Optically Stimulated Luminescence (OSL) results support earlier radiocarbon dates from the area. Moreover, an uplift curve constructed based on both types of dates concurs with a nearby uplift curve, indicating the potential of OSL for measuring uplift rates in this setting. Combining these datings with field observations enabled the calculation of process rates using field observations.” (P. 29, lines 743-747).

<u>List of relevant changes</u>

- The constructed uplift curve is changed to a quadratic relation between age and altitude. Consequently, the model parameters are recalculated and the model is rerun. Presented model results come from the new model run. They do not differ significantly relative to the results of the former manuscript.
- The chronological story is better elaborated on, with more detail on existing datings in the description of the study area.
- Soil data are presented more clear, with more detail on soil properties on different terrace levels.
- More explanation on the soil and horizon descriptions is provided, with more support for our choices to deviate from standard descriptions.
- More details are provided on the methodology for OSL dating.
- The abstract is revised and shortened.
- Statements in the Introduction and Discussion are better supported with relevant literature and references to the Results section.
- We have rephrased unclear sentences, where indicated.
- Our reconstructed uplift curve is compared in more detail with uplift curves reconstructed in surrounding areas.
- Conclusions on soil development and geochronology are reformulated.
- Several small changes to lay-out and syntax are made in the manuscript.

References

Dragon, K. and Marciniak, M.: Chemical composition of groundwater and surface water in the Arctic environment (Petuniabukta region, central Spitsbergen), Journal of Hydrology, 386, 160-172, 2010.

Gibas, J., Rachlewicz, G., and Szczuciński, W.: Application of DC resistivity soundings and geomorphological surveys in studies of modern Arctic glacier marginal zones, Petuniabukta, Spitsbergen, Polish Polar Research, 26, 239-258, 2005.

Long, A. J., Strzelecki, M. C., Lloyd, J. M., and Bryant, C. L.: Dating High Arctic Holocene relative sea level changes using juvenile articulated marine shells in raised beaches, Quaternary Science Reviews, 48, 61-66, 2012.

Rachlewicz, G. and Szczuciński, W.: Changes in thermal structure of permafrost active layer in a dry polar climate, Petuniabukta, Svalbard, Polish Polar Research, 29, 261-278, 2008.

Strzelecki, M. C.: High Arctic Paraglacial Coastal Evolution in Northern Billefjorden, Svalbard, Ph.D., Department of Geography, Durham University, Durham, 303 pp., 2012

Svendsen, J. I. and Mangerud, J.: Holocene glacial and climatic variations on Spitsbergen, Svalbard, The Holocene, 7, 45-57, 1997.

Vreeken, W. v.: Principal kinds of chronosequences and their significance in soil history, Journal of Soil Science, 26, 378-394, 1975.

Zwoliński, Z., Gizejewski, J., Karczewski, A., Kasprzak, M., Lankauf, K. R., Migon, P., Pekala, K., Repelewska-Pekalowa, J., Rachlewicz, G., Sobota, I., Stankowski, W., and Zagorski, P.: Geomorphological settings of Polish research stations on Spitsbergen, Landform Analysis, 22, 125-143, 2013.

Arctic soil development on a series of marine terraces on Central Spitsbergen, Svalbard: a combined geochronology, fieldwork and modelling approach

W. M. van der Meij[1,2], A. J. A. M. Temme[2,3], C. M. F. J. J. de Kleijn[2], T. Reimann[2], G. B. M. Heuvelink[2], Z. Zwoliński[4], G. Rachlewicz[4], K. Rymer[4], M. Sommer[1,5]

[1] Leibniz Centre for Agricultural Landscape Research (ZALF) e.V., Institute of Soil Landscape Research, Eberswalder Straße 84, 15374 Müncheberg, Germany

[2] Soil Geography and Landscape group, Wageningen University, P.O. box 47, Wageningen, Netherlands

[3] Institute for Alpine and Arctic Research (INSTAAR), University of Colorado, Boulder, Colorado

[4] Institute of Geoecology and Geoinformation, Adam Mickiewicz University, Poznań, Poland

[5] Institute of Earth and Environmental Sciences, University of Potsdam, 14476 Potsdam, Germany

Correspondence to: W.M. van der Meij (marijn.vandermeij@wur.nl)

Keywords: Spitsbergen, Svalbard, Arctic soils, luminescence dating, soilscape modelling, LORICA

Abstract

Soils in Arctic regions currently enjoy ~~significant~~ attention because of their ~~potentially substantial changes under~~ sensitivity to climate change. It is therefore important to ~~quantify~~understand the natural processes and rates of development of these soils~~, to better define and determine current and future changes.~~. Specifically, there is a need to quantify the rates and interactions between various landscape and soil~~-~~ forming processes~~ that together have resulted in current soil properties~~. Soil chronosequences are ideal natural experiments for this purpose. In this contribution, we combine field observations, luminescence dating and soil-landscape modelling to ~~test and~~ improve and test our understanding ~~about~~of Arctic soil formation. ~~Our~~The field site is a Holocene chronosequence of gravelly raised marine terraces in central Spitsbergen.

Field observations ~~suggest~~show that soil-landscape development is mainly driven by weathering, silt translocation, aeolian deposition and rill erosion. Spatial soil ~~heterogeneity~~variation is mainly caused by soil age, morphological position within a terrace and depth under the surface. ~~Substantial organic matter accumulation only occurs in few, badly drained positions.~~ Luminescence dating confirmed existing radiocarbon dating of the terraces, which are between ~~~3.6~~1.5 ka and ~~~14.4~~13.3 ka old. ~~Observations and ages were used to parametrize soil~~Soil landscape evolution model LORICA~~, which~~ was ~~subsequently~~ used to test ~~the~~our hypothesis that ~~our~~the field-observed processes indeed dominate soil-landscape development. Model results ~~indicate~~additionally indicated the importance of aeolian deposition as a source of fine material in the subsoil for both sheltered ~~beach~~and vegetated trough positions and barren ~~beach~~ ridge positions. Simulated overland erosion was negligible. ~~Therefore~~Consequently, an un-simulated process must be responsible for creating the observed erosion rills. Dissolution and physical weathering both play a major role. However, ~~by~~ using present day soil observations, the relative contribution of physical and chemical weathering could not be disentangled. Discrepancies between field and model results indicate that soil formation is non-linear and driven by spatially and temporally varying boundary conditions which were not included in the model. Concluding, Arctic soil and landscape development appears to be more complex and less straight-forward than could be reasoned from field observations.

1 Introduction

Soils in Arctic and boreal landscapes have recently ~~raised~~received intense research interest~~. This is~~, because the climate in these regions is expected to experience stronger changes than elsewhere (e.g. Arctic Climate Impact Assessment, 2004; Forland et al., 2011; Zwoliński et al., 2008). The effects of this increase are so far only partially understood (e.g. plant community development, Hodkinson et al., 2003). Another point of interest in the area is the poorly constrained Arctic carbon pool and its potential as carbon sink (e.g. Ping et al., 2008). To provide context to the short-term changes (~100 years) in Arctic and boreal soils that we are currently observing, knowledge on long-term soil development (~~~1000~~10.000 years) is urgently required as baseline~~. This suggests that~~: we need to better constrain the natural (i.e. paraglacial, Ballantyne, 2002; Slaymaker, 2011) processes, rates and feedbacks in the soil-landscape system. With such understanding, meaningful comparisons can be made between short-term rates of change in soils due to changing climate on one hand, and long-term rates of change in soils on the other hand.

Chronosequences are a popular means to obtain information about natural rates of soil formation (e.g. Birkeland, 1992; Egli et al., 2006; Phillips, 2015; Sommer and Schlichting, 1997). ~~In chronosequences, differences in properties of soils are attributed to differences in the age of those soils. This attribution is valid if other soil forming processes, such as landscape position, climate, lithology or organisms, do not vary between positions on the chronosequence. Ideally (but unusually), these factors are also constant over time.~~In chronosequences, the only soil forming factor that is significantly different for all soils is time. Variation in the other soil forming factors, i.e. landscape position, climate, lithology and organisms, is assumed equal for all soils in the study area. Consequently, variation in soil properties can mainly be attributed to the age of the soil (Vreeken, 1975). In Arctic regions, two paraglacial landscape settings are particularly suitable for chronosequences. Proglacial areas, where glaciers are currently retreating, are often used to compare soils formed at the onset of the recent retreat (~100 years ago) with those formed in very recently exposed glacial parent material. This can ~~provide~~illustrate decadal rates of soil formation (Egli et al., 2014; Kabala and Zapart, 2012). Another~~ successful~~ chronosequence setting is provided by series of marine terraces, also known as raised beaches, ~~reflecting~~which reflect millennial-scale isostatic rebound after the end of the Last Glacial Maximum. Such terraces are ubiquitous in

Arctic landscapes (Scheffers et al., 2012). Terrace chronosequences can provide millennial rates of soil formation, which is particularly helpful because natural soil formation in Arctic regions is relatively slow ~~and many differences become apparent only after thousands of years.~~ (Bockheim and Ugolini, 1990; Fischer, 1990) and many differences become apparent only after thousands of years.

~~Several factors nonetheless complicate the use of marine terraces to study rates of natural soil formation. First, a typical terrace consists of slight elevated ridge positions and somewhat lower trough positions~~Several factors nonetheless distort the temporal signal in chronosequences of marine terraces, as occurs more often in long-term chronosequences (e.g. Birkeland, 1990). First, a typical terrace consists of slight elevated ridge positions and lower trough positions (Pereverzev and Litvinova, 2010) and thus contains altitude differences resulting in different hydrological conditions that affect soil formation (Makaske and Augustinus, 1998; Scheffers et al., 2012). ~~Second, geomorphic processes may not only have a different effect on ridges and troughs, but also on terraces on different positions in the landscape – particularly when~~Second, geomorphic processes may not only have a different effect on ridges and troughs, but also on terraces at different positions in the landscape (Pereverzev and Litvinova, 2010) – particularly where a marine terrace complex is part of otherwise mountainous topography. Erosion and deposition can occur with different rates on different terrace levels~~.~~ (Strzelecki, 2012). Third, it is difficult to verify whether the composition and particle size distribution of soil parent material (beach deposits) at the onset of soil formation have been the same within and between terrace levels~~. In other words, the soil forming factors landscape position and parent material are not the same in all positions of the chronosequence.~~ (Mann et al., 1986). In other words, landscape position and composition of parent material may also have played a role in determining the present soil heterogeneity (Temme and Lange, 2014). These complications to chronosequences can lead to a problem of attribution: are observed differences between soils predominantly the result of a difference in age, or are other factors important as well?

The attribution problem can only be solved by using a combination of various methods. Clearly, geochronology is needed to provide accurate dating of the initiation of soil formation, and field and laboratory observations of soils are needed to determine properties of interest. However, in addition to these methods, model simulations of the various effects of ~~age~~time and other soil forming factors on soil development in a landscape context are ~~needed~~essential to determine which differences in soil forming factors may have caused differences in observations. A combination of these methods is thus needed to study long-term Arctic soil development that is not only influenced by time, but also by topographical position.

In this study, we focused on soils in a sequence of marine terraces in central Spitsbergen, Svalbard archipelago, to derive natural processes and rates of soil formation in a landscape context (Elster and Rachlewicz, 2012; Rachlewicz et al., 2013; Zwoliński et al., 2013). We first used Optically Stimulated Luminescence (OSL) dating to complement earlier experimental datings of juvenile marine shells on the same series of terraces (Long et al., 2012). Then, we performed field and laboratory analyses to describe soil properties in a variety of locations on the marine terrace complex. Together with dating results, this allowed us to calculate rates of some soil forming processes. Third, we used these rates to simulate combined soil-landscape development using a spatially distributed soil-landscape evolution model. Soil-landscape modelling has hitherto rarely been used in soil chronosequence studies (but see Sauer et al., 2012). However, by combining the various interacting geomorphic and pedogenic process, it allowed us to test and increase our understanding of interacting soil and landscape shaping processes in the study site. For simulations, we first hypothesized which soil-forming processes played a dominant role. Next, the recently developed soil-landscape evolution model LORICA (Temme and Vanwalleghem, 2015) was adapted to reflect this hypothesis. Model inputs and parameters were derived from field observations. Model outputs were compared to observations and conclusions were drawn with regard to the validity of our hypotheses.

2 Study area

2.1 Location and geomorphology

Fieldwork was conducted in the Ebba valley, one of the glacial valleys that enter Petunia Bay in the north tip of the Billefjorden, Central Spitsbergen (Svalbard archipelago, Fig. 1). A sequence of six marine terraces is located at the mouth of the valley, bordered by the Ebba river and floodplain to the north, alluvial material to the east and south and by the fjord to the west. ~~Prominent erosion rills and tundra lakes~~Prominent erosion rills and tundra lakes (Mazurek et al., 2012) were excluded from the study area (Fig. 1). The terrace sediments (i.e. soil parent material) dominantly consist of well-rounded gravel and coarse sand of limestone lithology, but gravel and sand from shale, sandstone and mafic intrusions are also found.

The area has been subject of research for many years (e.g. Gulińska et al., 2003; Kłysz et al., 1988; Kłysz et al., 1989; Long et al., 2012; Zwoliński et al., 2013). The marine terraces occupy a range of altitudes in the landscape~~,~~ (~1-50 m), due to isostatic rebound after the last Glacial. The typical, smooth ridge and trough morphology~~-~~ (Makaske and Augustinus, 1998; Scheffers et al., 2012) of terraces was formed by wave-action and sea-level fluctuations. Six terrace levels can be distinguished, each consisting of a smaller series of ridges and intermediate troughs. The oldest marine terrace in the series (terrace 6, Fig. 1) dates back to the Late Pleistocene (Kłysz et al., 1989), yet is very small and was not sampled in the present study. ~~There are no marine terraces younger than about 3000 years due to current relative sea level rise (Rachlewicz et al., 2013). Several lower terraces~~Terrace levels 1-4 have been dated using an experimental approach of radiocarbon dating of juvenile marine shells (Long et al., 2012)~~. The authors mentioned that a source of uncertainty in this method is the possibility of dating shells older than the terrace ridge they were found on. However, quality of their datings concurred to the more common method of radiocarbon dating of driftwood. Ages showed a clear trend with altitude.~~. The ages range from 3156±81 to 9718±91 years, suggesting that younger soils might have been flooded again (Strzelecki, 2012). Age increases continuously with increasing elevation. The approximate locations and individual ages of the datings of Long et al. (2012) are displayed in Fig. 1 and Fig. 3.

Due to their slightly more sheltered position and lower altitude relative to the smooth ridges, the troughs ~~reveal~~have denser vegetation. Ridge positions are in general free from vegetation~~.~~, but can be partly covered by bacterial soil crusts. In ~~the~~an aerial photograph from summer

2009, the barren ridges and terrace edges are characterized by lighter colours, whereas trough positions are characterized by darker colours (Fig. 1)

Location of Figure 1.

2.2 Arctic soils

Most soils of Spitsbergen have formed in coastal settings. Soils typically have shallow profiles with poorly differentiated genetic horizons~~,~~ of sandy or loamy texture, pH-values varying between 7 and 8 and organic carbon contents from 0 up to ~~4~~10% (Melke and Chodorowski, 2006; Pereverzev, 2012). In some cases, soils have been affected by geomorphic activity such as cryogenic processes and erosion (Lindner and Marks, 1990). Thickness of the marine deposits is between 1-2 meter (Zwoliński et al., 2013). Soils formed in those deposits are well developed compared to proglacial soils, but are nonetheless mainly described as incompletely developed soils (Cambisols, Cryosols, Leptosols, Regosols, Kabala and Zapart, 2009). In the Ebba valley, the thickness of the active layer varies between 0.3 and 2.5 m (Gibas et al., 2005), with thaw depths ranging from 0.45 to 1.2 m on the marine terraces (Rachlewicz and Szczuciński, 2008).

The dominantly mentioned soil forming processes are: weathering~~-~~ through frost action and dissolution (Forman and Miller, 1984; Kabala and Zapart, 2009), calcification (Courty et al., 1994; Ugolini, 1986), silt eluviation (Forman and Miller, 1984) and the formation of organic matter (Melke, 2007). Especially the process of silt eluviation is typical for the coarse-grained Arctic soils. Forman and Miller (1984) identified six stages of silt eluviation, which indicate an increasing presence of silt caps on top of clasts for stage 1-4. In stage 5 and 6 the individual silt caps connect and fill the space between the clasts, eventually leading to a matrix-supported soil. The presence of silt caps is associated with coarse-grained and well drained soils (e.g. Locke, 1986; Ugolini et al., 2006), dense vegetation capturing aeolian silt (Burns, 1980, as stated in Forman and Miller, 1984), illuviation by precipitation (Locke, 1986) and vertical frost sorting (Bockheim and Tarnocai, 1998).

2.3 Climate

The study area has an average annual temperature of -5°C, with average temperatures in summer and winter ~~are~~of +6 and -15°C respectively (Przybylak et al., 2014). The average annual precipitation is 150-200 mm, mainly as snow ~~fall~~ (Láska et al., 2012; Rachlewicz and

Szczuciński, 2008; Rachlewicz et al., 2013). The climatic conditions are more extreme compared to the western coast of Spitsbergen, with warmer summers, colder winters and ~~general aridity~~less precipitation (Przybylak et al., 2014; Rachlewicz, 2009). The climate is classified as an Arctic Desert or Tundra (ET, Köppen, 1931).

The prevailing wind directions in the Ebba valley are south or northeast with the strongest winds (>6 m/s) blowing from the Ebba glacier in the northeast (Láska et al., 2012). These strong winds in combination with scarce vegetation and a high availability of sediments on the sandur plains ~~leads~~lead to active wind erosion and ~~eventually~~subsequently to downwind accumulation of aeolian sediments. Deposition occurs when wind speed decreases or when the sediments get mixed with falling snow in autumn and winter, also known as niveo-aeolian deposition (Rachlewicz, 2010). In the Ebba valley plants are a good indicator of hydrological and soil characteristics, yet reflect the cold climate. Hydrophilic species are found in wet trough positions whereas vascular species were sporadically found on better drained and better developed soils on ridges (Jónsdóttir et al., 2006; Prach et al., 2012). Vegetation cover in the study area is around 30% (Buchwal et al., 2013).

3 Methods

3.1 Luminescence dating

To complement the experimental rebound chronology from Long et al. (2012), we applied OSL dating to samples ~~of~~taken from the sand fraction of the marine sediments from terrace levels 1, 3 and 5 in the study area (Fig. 1~~).~~). The samples were collected at a depth of 0.27 or 0.57 meters from pits dug in the marine sediments (Table 2) and were shielded from light. The fine sand fraction (180-250 µm) of marine sediments can be assumed to be well bleached, due to reworking by wave action in the swash zone (Reimann et al., 2012). Nonetheless, to account for the possibility of insufficient signal resetting, termed partial bleaching, we applied the single-aliquot regenerative-dose (SAR) measurement protocol of Murray and Wintle (2003) and made use of a small aliquot approach (e.g. Reimann et al., 2012; Rodnight et al., 2006).

Two quantities are determined for OSL dating. First, measurement of the OSL signal on the purified quartz mineral fraction reveals how much ionizing radiation the sample received since the last bleaching event (i.e. prior to burial). Second, this measurement is combined with a measurement of the background radiation level at the sample position. The luminescence age (ka) is then obtained by dividing the amount of radiation received (palaeodose, Gy) by the rate at which this dose accumulates (dose rate, Gy/ka):

$$\text{OSL age (ka)} = \text{Palaeodose (Gy)} / \text{dose rate (Gy/ka)} \tag{1}$$

The basic principles of OSL dating are reviewed in (Aitken, 1998) and (Preusser et al., 2008).

For dose rate estimation we used high-resolution gamma ray spectrometry. Activity concentrations of ^{40}K and several nuclides from the Uranium and Thorium decay chains were measured. Results were combined with information on geographic location and burial history (Prescott and Hutton, 1994), water and organic content history (Aitken, 1998; Madsen et al., 2005). Furthermore, grain size dependent attenuation effects were incorporated (Mejdahl, 1979) ~~-~~to calculate the effective dose rate. The total dose rate is listed in Table 2.

For the OSL measurements the three sediment samples were prepared in the Netherlands Centre for Luminescence dating under subdued orange light conditions. The samples were sieved to obtain the 180-250 µm grain size fractions which were subsequently cleaned using HCl (10 %) and ~~H_20_2~~H_2O_2 (10 %). Grains of different minerals were separated from each other using a heavy liquid (LST). The quartz-rich fraction (ρ > 2.58 g~~/cm^3~~ cm^{-3}) was then etched with 40 % HF for 45 min to remove remaining feldspar contamination and the outer rim of the quartz grains. The purified quartz fraction was again sieved with a 180 µm mesh to remove particles that had become too small by etching.

To estimate the palaeodose of the samples, the OSL from quartz was measured by applying the ~~single-aliquot regenerative-dose (SAR) measurement protocol of Murray and Wintle (2003).~~SAR protocol. The most light-sensitive and most suitable OSL signal of the quartz grains was selected using the 'Early Background' approach (Cunningham and Wallinga, 2010). To obtain a good estimate of the palaeodose, measurements were repeated on at least 28 subsamples (aliquots) per sample. Each aliquot consisted of 40-70 grains. To test the SAR procedure, a dose recovery experiment was then carried out on four aliquots of each sample. The average recovered dose agreed with the laboratory given dose. The ratio of measured dose divided by given laboratory dose was 0.96±0.02 (n = 11~~)~~), confirming the suitability of the selected measurement parameters.

The ~~single-~~small aliquot palaeodose distributions were symmetric and moderately scattered. We calculated over-dispersion values, i.e. the scatter in the palaeodose distributions that cannot be explained by the measurement uncertainties (Galbraith et al., 1999), to be between 12±3 % and 33±9 %. These over-dispersion values are typical for well-bleached sediments derived from coarse-grained marine deposits (e.g. Reimann et al., 2012). Furthermore, the over-dispersion increased with age suggesting that it is unlikely that partial bleaching is the source of the unexplained scatter. Therefore, palaeodoses of our samples were derived from the single-aliquot palaeodose distributions by applying the Central Age Model (CAM, Galbraith et al., 1999).

3.2 Soil observations

The study area was divided into three equally sized strata based on altitude, which in turn were divided into vegetated (trough) and non-vegetated (ridge) sub-strata using the aerial photograph~~ from summer 2009. 30~~. Thirty random locations were divided over the six strata according to stratum size, with at least 2 locations in each stratum (Fig. 1). ~~11~~8 pits were located on ridge positions and ~~19~~22 pits on trough positions.

Soil profiles were mostly described according to FAO standards ~~(FAO, 2006; IUSS Working Group WRB, 2014). Additionally, the B*l*~~(FAO, 2006; IUSS Working Group WRB, 2015). We deviated from the standard horizon designation in three ways, because that allowed easier comparison between different soils and because it better suits the locally observed soil properties. The deviations are: 1) All aeolian horizons were recorded with prefix 1, whereas all horizons developed in marine parent material were recorded with prefix 2, also the ones without aeolian cover. This was done to easily distinguish between different parent materials. Additionally, where present, we always described the aeolian cover as one horizon. The cover had traces of organic matter throughout the whole horizon and was therefore classified as 1AC horizon. 2) Marine horizons buried below an aeolian cover were not assigned the typical 'b' suffix for buried horizons. This facilitated grouping of comparable horizons independent of morphological position. In the same way we did not include the suffix 'k' for horizons with secondary carbonates, although these were present in most subsurface marine horizons and partly in marine A horizons. 3) As silt enriched horizons occurred in most soil profiles, the B*l* horizon classification as proposed by Forman and Miller (1984)~~, was used for layers with substantial silt illuviation. To easily distinguish between different parent materials, aeolian horizons were recorded with the prefix 1, whereas horizons developed in parent marine material were recorded with the prefix 2. This was done even when marine material was not overlain by aeolian material (Fig. 4).~~

~~We classified soils purely based on field observations. In most (well drained) positions, this meant that we were unable to determine whether the conditions for a Cryic horizon were met. In these cases, we assumed horizons were not Cryic.~~ was used to distinguish these horizons. The lower case italic L (*l*) indicates the pedogenic accumulation of silt. This designation was only applied when silt was not only present on top of the clasts, but also filled the matrix. These horizons conform to stage 5 or 6 in the silt morphology classification of Forman and Miller (1984). The three deviations mean that two typical soil profiles in the area (e.g. Fig. 4) were described as 1AC-2A-2B*l*-2BC and 2A-2B*l*-2BC instead of the formal 1Ah-1ACh-2Ahb-2Bkb-2BCkb and Ah-Bk-BCk.

Soil pits were dug until the unaltered parent material was reached or until further digging was not possible. Each major soil horizon was sampled. Bulk density was measured in the field using a 100 cm^3 bulk density ring. For horizons with predominantly gravel, it was not always possible to completely fill the ring by hammering it into the soil. In these cases, the bulk density ring was manually filled up with soil material, which may have led to an underestimation of bulk density. Field bulk density measurements were corrected for the moisture content, which was determined by drying samples overnight at 105 °C. Samples were subsequently dry sieved into three grain size fractions: gravel (> 2 mm), sand (2 mm – 0.063 mm) and silt and clay (< 0.063 mm). Organic matter content was determined by loss on ignition. Samples were heated to 550 °C for three hours.

~~The effects of soil horizon, terrace level and terrace morphological setting (ridge / trough) on the soil properties were assessed using a three-factor analysis of variance (ANOVA). A linear model was used to explain variation using the three factors.~~

A three-factor ANOVA without interactions was used to test the effect of explanatory variables (terrace level, morphological setting and horizon type) on dependent variables (gravel fraction, sand fraction, organic matter fraction and the logarithm of silt fraction). The use of ANOVA was justified, as the Shapiro-Wilk test indicated a normal distribution of the residuals of a linear model between all explanatory variables and the individual dependent variables. The linear model was used to explain which part of the variation in soil properties could be attributed to each of the explanatory variables.

3.3 Soilscape model LORICA

Soilscape model LORICA was used to simulate joint soil and landscape development. This raster-based model simulates lateral geomorphic surface processes together with vertical soil development (Temme and Vanwalleghem, 2015, Fig. 2). Transport and change of sediments and soil material are based on a mass balance of various grain size classes.

The model setup that was used in this study contained 10 soil layers in every raster cell of 10 m x 10 m, each with an initial thickness of 0.15 m each. This created an initial thickness of marine sediments (the soil parent material) of 1.5 ~~meters~~m. Only three grain size classes were simulated: gravel (> 2 mm), sand (2 mm – 0.063 mm) and the combined silt and clay class, from now on called silt (< 0.063 mm).

~~During~~In model simulations, ~~the~~ different processes ~~can~~ change the mass of material in each grain size class in each soil layer. Using a bulk density pedotransfer function, this change in mass and composition of soil material is translated to a change in layer thickness and a corresponding change in surface altitude. Geomorphic processes are oriented laterally and only affect the top soil layer~~ of each cell, while soil forming~~. Pedogenic processes are oriented vertically and alter ~~and~~material or transport material ~~in a vertical direction between layers.~~ from one soil layer to another. Some of LORICA's original soil process formulations were adapted to match our hypothesis of the main processes occurring in marine terraces. Some other processes were assumed less relevant, based on literature and exploratory fieldwork. Hence, they were deactivated for this study.

Chemical weathering was also not activated. However, it is important to note that chemical weathering in the form of dissolution does occur in the marine terraces (Mazurek et al., 2012) and constitutes a source of sand and silt in Arctic soils elsewhere (reported from the west of Spitsbergen, Forman and Miller, 1984; Ugolini, 1986). However, it is not clear to which extent dissolution contributes to in situ weathering on the marine terraces specifically, where physical weathering also plays a dominant role. Only physical weathering was activated in LORICA. Since dissolution mainly focuses on fine material (Courty et al., 1994), a possible overestimation of the finer fractions, relative to the coarse fractions, would be an indicator of the importance, and could possibly hint at the rate, of dissolution.

Location of Figure 2.

3.3.1 Model framework

A DEM with a cell size of 10 m x 10 m served as input landscape. For trough positions, the thickness of the ~~1A~~1AC horizon following from a trend with age was subtracted from the DEM to simulate ~~initial conditions.~~altitude before aeolian deposition started. A part of the upslope area was included in the DEM to ~~enable import~~allow simulation of transport of sediments into the study area. Climatic data required by LORICA are annual precipitation and evapotranspiration. As we did not have data on the paleoclimate of the study area, we assumed a constant precipitation and evapotranspiration over the entire model run. The same goes for rates and parameters of the simulated processes (Table 1). Annual precipitation is 150-200 mm (Rachlewicz, 2009; Rachlewicz et al., 2013; Strzelecki, 2012). We assumed that a large fraction is lost to infiltration, evaporation and sublimation, leaving 50 mm for overland flow. The initial composition of the marine parent material was derived from field observations and is ~~90~~95% gravel with ~~10~~5% sand.

To reflect isostatic rebound, a growing part of the landscape was exposed to process calculations as time progressed. ~~Results~~Our results from geochronology of ~~marine~~the terraces were used to inform this. Simulations started at the time when terrace level 6 was completely above water ~~-~~and progressed with an annual timestep. Cells outside the study area (Fig. 1) were not included in simulations.

The activated processes and modifications to them are described below. Where applicable, the calculation of parameter values is also described.

Location of table 1.

3.3.2 Geomorphic processes

LORICA generates run-off and infiltration by applying precipitation and snow melt to the grid cells. Run-off flows downhill, potentially eroding and collecting sediment on its way. ~~When~~Deposition starts when the amount of transported sediment surpasses the sediment transport capacity of the water~~, deposition starts. Sediments can be~~. Undeposited sediment is transported out of the study area to the Ebba river and Petunia bay. Vegetation protection and surface armouring by coarse grains decrease the mass of material that can be eroded. A more extensive explanation of this landscape process is provided in Temme and Vanwalleghem (2015). Standard parameter values were used for almost all parameters describing this process, except for the vegetation protection constant. This dimensionless parameter was set from 1 to 0.5 because of the scarce vegetation in the study site.

For aeolian deposition, a simple linear process description was implemented that added a constant amount of aeolian material to all cells in trough positions for every timestep. Ridge positions received no aeolian deposition. The aerial photograph (Fig. 1), aggregated to the raster cell size of the input DEM of 10 m, was used to distinguish between ridge and trough positions.

The annual volume of aeolian deposition per cell surface (m^3 m^{-2} ~~y~~a^{-1}, or m ~~y~~a^{-1}) was calculated by regressing observed aeolian (~~1A~~1AC) horizon thickness to soil age. ~~Bulk~~The bulk density of aeolian deposits, undisturbed by current vegetation, was measured in the field and used to convert the volume to mass. The initial grain size distribution of aeolian deposits was calculated by extrapolating trends in sand and silt fractions of ~~1A~~1AC horizons with age to timestep 0.

3.3.3 Pedogenic processes

Pedotransfer functions are used to estimate unknown variables from readily available soil data (McBratney et al., 2002).. Because LORICA's original pedotransfer function for bulk density (BD_l, ~~kg m~~g cm^{-3}) is unsuitable for clast-supported soils, we estimated a new pedotransfer function based on the gravel and sand fractions and depth under the soil surface ~~of a soil layer.~~(m). Soil horizons from both marine and aeolian parent material, where bulk density and particle size distribution were known (n=62), were used to estimate the parameters of this function (Eq. 2). The pedotransfer function was validated using leave-one-out cross-validation on the 62 soil horizons (RMSE~~=~~ = 0.183 ~~kg m~~g cm^{-3}~~, R^2 = 0.25~~).

$$BD_l = \cancel{99 + 1212}\, 0.099 + 1.212 * gravel_{frac,l} + \cancel{1283}\, 1.283 * sand_{frac,l} + 0.353 * depth_l \tag{2}$$

Physical weathering in LORICA for the various grain size classes i is described as:

$$\Delta M_{pw\ i,l} = -M_{i,l}\, C_3\, e^{C_4\, depth_l}\, \frac{C_5}{\log size_i} \tag{3}$$

where the change in mass due to physical weathering ΔM_{pw} in layer l is a function of the mass present in the grain size class $M_{i,l}$, depth below the surface $depth_l$ and the median grain size of the fraction $size_i$ ~~-~~(Temme and Vanwalleghem, 2015). With parameter C_5 at its standard value of 5, weathering increases with increasing grain size. ~~Weathering rate C_3 and depth-decay parameter C_4 were parameterized from field data.~~

Weathering rate C_3 and depth-decay parameter C_4 were parameterized from field data. To calculate these parameters, we assumed that a change in gravel fraction in the subsoil is only due to physical weathering. In contrast, topsoil horizons were assumed to be also affected by geomorphic processes. First, weathering rate C of gravel in 2B*l* and 2BC horizons was derived from the decay in gravel fraction using:

$$\log(gravel_{t,l}) = \log(gravel_{0,l}) - C_{gravel,l} * t \tag{4}$$

~~With~~with $gravel_{t,l}$, $gravel_{0,l}$ and $C_{gravel,l}$ as gravel fraction at time t (-), initial gravel fraction (-) and weathering rate of gravel in horizon l (~~y^{-1}) respectively.~~ a^{-1}) respectively. The log function in Eq. (4) followed from Eq. (3), where weathering results in an exponential decay of the mass of a certain grain size class.

Second, depth decay parameter C_4 was derived using the differences in weathering rates and average depths between the B*l* and BC horizons.

With the depth decay constant C_4, the weathering rate at the soil surface ($C_{gravel,0}$) was derived, and weathering rate C_3 was calculated using Eq. (3).

Silt translocation was simulated using LORICA's formulation for clay eluviation (Temme and Vanwalleghem, 2015), but a depth decay factor was introduced to better simulate the belly shape of the silt profiles in the soil.

The values for the maximum silt eluviation in a completely silty sediment, and the depth decay factor were determined using manual inverse modelling (i.e. through model calibration), using 40 runs with different parameter values. Simulated silt profiles were compared with observed silt profiles for four representative soil profiles in the field (profiles 3, 6, 10 and 24). The objective function for calibration was to minimize the average Root Mean Squared Error between the modelled and simulated silt fraction for 5 cm thick layers over the entire depth of the profile.

3.4 Model validation

Model results were validated using site- and horizon-specific field observations of the gravel, sand and silt fraction, matched to their ~~respective~~ location in the simulated soilscape. Because of the small amount of observations, also observations used for parameterization and calibration were used in the validation. ~~These observations were used for only one of the processes, whereas validation happens over the results from all processes simulated together.~~

The mean prediction error (ME) was calculated to assess a bias between field measurements and model results. The root mean squared error (RMSE) was calculated to measure the difference. Normalized ME (ME_n) and RMSE ($RMSE_n$) were calculated by dividing the ME and RMSE by the average observed value (Janssen and Heuberger, 1995). For the mass fractions this was done for every profile, over the depth of observations available for that profile. For the mass content this was done by considering locations on a certain morphological position together.

4 Results

4.1 Geochronology

Location of table 2.

The three OSL samples taken in the marine sediments show increasing age with increasing terrace level (Fig. 1, Table 2). Datings of the first main terrace level show an age of 4.4 ± 0.2 ka. The highest part of terrace level 3 has been dated to 7.3 ± 0.4 ka. Terrace level 5 dates ~~back~~ to 12.8 ± 1.1 ka.

Location of Figure 3.

These results support the radiocarbon datings of Long et al. (2012) that covered terrace levels 1 to 4 (Fig. 1). The combined sets of ages (a) show a clear relation with altitude ~~(~~(m), which we approximated with a quadratic trend (Fig. 3~~). This trend, 229 years for every meter of uplift, was used to inform isostatic rebound in LORICA (Fig. 3). The offset of the regression suggests that the youngest soils that are older than the present beach, are approximately 3630 years old. The youngest soils on terrace level 6 are 14393 years old. This age was hence used as the start of our model simulations, where terrace level 6 was completely above water.~~):

$$altitude = 2.69 * 10^{-7} * age^2 - 0.64 \quad (5)$$

This trend was used to inform isostatic rebound in LORICA. The offset of the trend suggests that the youngest soils are approximately 1500 years old. Following the trend, the youngest soils on terrace level 6 are 13300 years old. This age was hence used as the start of our model simulations, when terrace level 6 was completely above water. The age ranges of the different terraces, minimum and maximum elevation of each terrace and Eq. 5, increase with altitude (Table 3). However, there is some overlap in ages of different terraces.

4.2 Soil types and properties

Location of Figure 4.

~~Ridge~~Although all observed soils can be classified as Cryosols, there are still distinct differences between ridge (8 soils) and trough (22 soils) positions~~ show distinct soil types.~~. Ridge positions are generally well drained and ~~therefore~~ usually contain ~~Episkeletic Calcisols (observed 9 times), unless at a more moist position, where they developed into Skeletic Turbic Cryosols (2). Soils in a beach trough are often Endoskeletic Rendzic~~skeletic Cryosols

(~~11), unless they are atypically dry (Skeletic Calcisols (2) or atypically wet (Abruptic Phaeozems (2). In the oldest terraces, trough soils are Abruptic Chernozems (4), created by bacterial and fungal breakdown of organic material, which is later transported through the soil.~~observed 7 times). All ridge soils have accumulated secondary carbonates (calcic). Trough soils are typically vegetated and therefore capture aeolian sediment which forms into an aeolian ~~A~~AC-horizon, which is rarely present on ridges (Fig. 4~~). ~~). The aeolian cover displays darker colours due to moderate content of organic matter in 16 trough soils. Younger trough soils are skeletic, due to their thinner aeolian cover and less weathered 2A horizons (6 times). Older soils display an endoskeletic horizon (12 times). For 4 trough soils, the skeletic properties are absent, due to very thick combined A horizons. Cryoturbation features like frost heave and patterned ground were visible in some trough positions.

Location of table 3.

In general, sand and OM fraction decrease towards deeper lying horizons~~.~~ (Table 3, Fig. 5). OM shows small variation, considering the standard ~~deviation~~deviations. Silt fraction shows ~~a maximum~~the highest values in 2A horizons, and ~~afterwards decreases~~is lower in lower lying horizons. The decrease of silt fraction in 1AC and 2A horizons and increase of silt fraction in 2B*l* horizons with increasing ~~depth. Consequently, the relative amount of gravel increases (Table 3).~~terrace level (Table 3, Fig. 5) indicate transport of silt from surface layers to lower lying layers. This was also evident from field observations, where silt caps were located on clasts in the subsoil and the 2B*l* horizons showed an enrichment of silt throughout the whole horizon (Fig. 4). This enrichment was not homogenous, as occasionally bands of higher silt content could be identified inside the 2B*l* horizons. Carbonate content also increases with depth. Aeolian horizons are moderately calcareous. Conversely, gravelly marine horizons ~~appear to be~~are extremely calcareous, while the finer textured 2A horizons show a moderate to strong $CaCO_3$ content, which indicates loss of carbonates. The fine ~~1A~~1AC horizons show a relatively high bulk density, compared to 2A horizons~~.~~ (Table 3, Fig. 5). Average bulk densities increase with depth in marine sediments. The detailed field descriptions show a large variation in ~~BD~~bulk density inside ~~1A horizons~~the aeolian cover. Buried aeolian deposits, without observed humus content, have a bulk density of 1651 ± 240 kg m^{-3}.

Location of Figure 5.

Nonetheless, part of the variation within soil profiles is explained by soil horizon and terrace level (Fig. 5). The three-factor ANOVA confirms the significant effect ($P<0.05$) of the soil horizon and terrace level, as well as morphological setting on the variation in gravel and sand fraction. On the contrary, terrace level was not a significant explanatory variable for variation in the log-silt and organic matter fraction. Here only soil horizon and morphological setting were significant in explaining part of the observed variation. A linear model involving all three factors resulted in adjusted R^2 of 0.~~83~~82, 0.~~85~~84, 0.~~42~~55 and 0.~~51~~52 for gravel, sand, log-silt and organic matter fraction respectively.

4.3 Process parameters

Slope of the linear regression between ~~1A~~1AC horizon thickness and age is ~~1.89~~2.41*10^{-5} m ~~y~~a^{-1} (R^2=0.~~29).~~33, p-value = 0.007). Multiplying this with bulk density of buried aeolian material gives a deposition rate of 0.~~031~~040 kg m^{-2} ~~y~~a^{-1}. Initial sand and silt fraction of the aeolian deposits are 84% and 16% respectively.

~~The~~Following the procedure described in Section 3.3.3, the calculated physical weathering rate of gravel at the surface ($C_{gravel,0}$) is ~~4.06~~3.25*10^{-5} kg kg^{-1} ~~y~~a^{-1}. This corresponds to a weathering rate *C3* of 1.~~26~~01*10^{-5} kg kg^{-1} ~~y~~a^{-1}, when considering the size-dependent correction factor. The corresponding depth decay constant C_4 is -~~2.22~~1.63 m^{-1}, which means that weathering rate decreases with about ~~90~~80% per meter under the soil surface.

Calibration of silt eluviation resulted in a maximum eluviation of 0.15 kg and a depth decay factor of ~~6~~5 m^{-1}.

4.4 Simulated landscape and soils

Model results show that the only significant changes in altitude besides uplift are due to aeolian deposition, with a maximum deposition of 0.~~45~~48 m, divided over ~~1A~~1AC horizons of max ~0.3 m and silt that eluviated from them into lower horizons, contributing the other ~0.15 m. ~~Changes in altitude caused by bulk density changes due to physical weathering are maximum 0.01 m.~~ Simulated altitude change due to erosion and sedimentation is negligible, with amounts of several millimetres. Altitude changes are larger on older terraces. There is a clear distinction between changes for trough and ridge positions, because the latter did not receive aeolian input (Fig. 6).

Location of Figure 6.

Variation in simulated profile curves of different particle sizes is mainly caused by morphological position of the soils (Fig. 7). Although the general shapes of these profiles correspond with the mean observed profiles, observed profile curves show a larger spread than simulated profile curves. Observed gravel fractions are lower than simulated fractions. Sand and silt fractions and mass were larger in the field than in the model results (Fig. 8). The silt fraction in the ~~top soils~~topsoils on both ridge and trough positions is higher in the field than in the model results.

Location of Figure 7.

Most accurate predictions for sand and silt fractions and contents are for trough positions (Table 4, Fig. 8). For gravel, ridge positions are predicted most ~~accurate~~accurately. The relatively high $RMSE_n$s indicate that there is a large spread between modelled and observed mass fractions and contents (cf. Fig. 7). On the other hand, ME_ns indicate a low bias in some of the predictions. Examples are sand and silt properties in trough positions, gravel and sand properties in ridge positions and total mass of soil material in all positions. The positive ME_n for total mass of the soil shows that the model slightly overestimates the amount of material in the soil. Sand and silt masses and fractions are generally underestimated.

Location of table 4.

Location of Figure 8.

In some places, the morphological position as derived from the aggregated aerial photograph and used in the model differs from field-observed morphological position~~.~~, due to small-scale variation between ridge and trough positions. These ‘mixed’ positions (Table 4 and Fig. 8) show the highest differences between observations and simulations and cause the largest errors in the validation statistics. Small differences between RMSE and ME for the mixed positions indicate that the largest part of the error is systematic, and a relatively small part is caused by a random error.

5 Discussion

5.1 Geochronology and isostatic rebound

Our new OSL dates and the existing calibrated radiocarbon results from Long et al. (2012) show comparable results for the ages of marine terraces in our study area. The ~~combined set of ages~~altitude above current sea level can be rather well approximated ~~through~~by a ~~linear relation~~quadratic equation with ~~altitude above current sea level, which gives~~age (Eq. 5). The uplift ranges from 7.2 mm a^{-1} 13300 years ago (altitude = 47 m) down to 0.8 mm a^{-1} 1500 years ago (altitude = 0 m), with an average ~~uplift~~ rate of 4.~~3~~0 mm ~~y~~a^{-1} ~~(R^2 = 0.966,~~ .(Fig. 3~~).~~ ~~The nearby Kapp Eckholm (location 23 in Forman et al., 2004) shows an average uplift rate over the last 9000 years of 5 mm y^{-1}. This is in the same order of magnitude as the average uplift rate found in this study. However, Kapp Eckholm shows a large decrease in uplift rates, from 12.5 mm y^{-1} (9000-7000 years ago) to 2 mm y^{-1} (5000 years to present). This was not apparent in our data. On the contrary, when considered individually, each set of dates suggests an increasing uplift rate over time. This provides an interesting counterpoint to the clear slowing down and reversal of uplift rates observed over all of Svalbard (Forman et al., 2004). The minimum age of the terraces of ~3.6 ka corresponds to the initiation of tide-water glaciers between 4 and 3 ka ago in response to the Holocene cooling, which eventually led to the Little Ice Age~~ (Svendsen and Mangerud, 1997b)~~. Apparently the uplift in the Ebba valley did slow down and eventually stop in response to renewed glacier growth. The terraces formed during decreased uplift rates could have been submerged again by renewed isostatic depression and late Holocene sea level rise (Zwoliński et al., 2013).~~). The age ranges of the different terraces show some overlap (Table 3). This is due to differences in elevation between ridge and trough positions, lower lying rills and inaccuracies in the DEM.

~~OSL ages have in general a larger uncertainty interval than the radiocarbon ages (Fig. 3), because OSL methods provide a lower precision than radiocarbon dating, especially in the age range of interest for this study. The typical OSL uncertainty is 5 to 10 % for the 1-sigma confidence interval (~65 %), which was also achieved for the samples under investigation. However,~~Forman et al. (2004) reviewed uplift rates of studies all over Svalbard. For every reviewed uplift curve, total uplift (m) at 9000, 7000 and 5000 uncalibrated radiocarbon years were supplied. In order to work with calibrated radiocarbon ages, the marine reservoir effect of 440 years (Forman et al., 2004) was added to these uncalibrated ages. Next, the ages were calibrated with CALIB 7.0.4 (Stuiver and Reimer, 1993), using the MARINE13 calibration curve (Reimer et al., 2013) . Uncertainty of the uncalibrated ages was assumed to be 1% (Walker, 2005, p. 23). The deviation from the standard marine reservoir effect (ΔR) was assumed to be 100±39 years (Long et al., 2012). The corresponding calibrated ages are 10157, 7808 and 5690 years BP. Because abovementioned assumptions and uncertainty in the estimation of the marine reservoir effect, the following analysis should be considered with caution.

From the calibrated ages, uplift rates over the last 10157 years, 10157-7808 years ago, 7808-5690 years ago and 5690 years to present could be calculated. Two of the reviewed uplift curves were located near the Ebba valley: Kapp Ekholm and Blomesletta (Péwé et al., 1982; Salvigsen, 1984) . For Kapp Ekholm, the uplift rates over these time intervals were 4.4 mm a^{-1}, 10.6 mm a^{-1}, 4.7 mm a^{-1} and 1.8 mm a^{-1}. For Blomesletta they were 2.5 mm a^{-1}, 5.5 mm a^{-1}, 2.4 mm a^{-1} and 1.2 mm a^{-1}. In comparison, uplift rates for these time intervals for our uplift curve were 2.7 mm a^{-1}, 4.7 mm a^{-1}, 3.8 mm a^{-1} and 1.4 mm a^{-1}. Uplift rates in the Ebba valley are thus very comparable to the Blomesletta uplift curves. The rates found at Kapp Ekholm are much higher. This discrepancy can be due to a large uncertainty in the uplift rates, which is not incorporated here. Nonetheless, the uplift curve from this study can be considered reliable, as the independent OSL ages support the earlier radiocarbon ages.

The fitted uplift curve suggests that the youngest terrace is around 1500 years old. That could indicate that uplift has stagnated or reversed, leading to flooding of lower lying terraces, as is also suggested by Long et al. (2012) and Strzelecki (2012). This corresponds to renewed glacier growth in response to a cooler climate starting 3000 years ago, which eventually led to the Little Ice Age (Rachlewicz et al., 2013; Svendsen and Mangerud, 1997a). The exact age of the youngest soils remains uncertain. However, the silt and organic matter profiles of the soils on terrace level 1 (Table 3, Fig. 5) nonetheless suggest that they have been developing for a longer time, instead of just having recently emerged from the sea. ~~OSL provides direct depositional ages of sand-sized marine deposits and can be used to independently validate the radiocarbon chronology. In our case both data sets agree and thus support each other.~~

A well-known disadvantage of radiocarbon dating is that older ages (>35 cal. ka) can easily be underestimated by contamination with ~~more modern~~younger carbon (Briant and Bateman, 2009). This may be the case with the radiocarbon dating of the highest terrace in the Ebba valley (>37000 years ago, Kłysz et al., 1989), but is unlikely for the Holocene terrace sequence that was studied in this paper. More importantly, radiocarbon ages derived from marine fauna (e.g. shells) needs to be corrected for the marine reservoir effect. However, this correction does not only require extra analysis (e.g. Long et al., 2012), it typically also shows a large regional ~~variety and thus potential bias. Another common problem of radiocarbon dating, especially in our geomorphological~~and biological variety and thus potential bias (Forman and Polyak, 1997). Another common problem of radiocarbon dating, especially in our geomorphologically very dynamic setting, is re-working of the dated material (e.g. Long et al., 2012). In this case the radiocarbon age might potentially overestimate the deposition age of the marine terrace. OSL does not suffer from these potential malign effects, as OSL provides direct depositional ages of sand-sized marine deposits and can be used to independently validate the radiocarbon chronology. In our case both data sets agree and thus support each other. ~~of the marine terrace. OSL does not suffer from these potential malign effects. On the other hand, OSL has already been successfully used~~OSL ages have in general a larger uncertainty interval than the radiocarbon ages (Fig. 3), because OSL methods typically provide a lower precision than radiocarbon dating. The typical OSL uncertainty is 5 to 10 % for the 1-sigma confidence interval (~65 %) (Preusser et al., 2008), which was also achieved for the samples under investigation. Furthermore, OSL is a well-established method to date recent coastal dynamics ~~(Ballarini et al., 2003; Reimann et al., 2010)~~ and aeolian activity (e.g. Sevink et al., 2013). Thus, when considering chronosequences with a longer age span and where recent geomorphic activity plays a role, OSL ~~is a good way to~~can validate radiocarbon chronologies and is a powerful alternative dating method.

5.2 Landscape evolution

It was our intention to use the LORICA model to test our field-informed hypotheses about the combined evolution of soils and landscapes in the study area. The aspects that were not well simulated, ~~can~~ therefore suggest improvements to process understanding.

The main geomorphic aspect that was not well simulated, is the presence of small rills incising into the smooth terrace ridges (Mazurek et al., 2012). These were observed on all terrace levels, but not simulated (Fig. 1 and Fig. 6). Model tests indicate that ~~unrealistic~~unrealistically high erodibility values would have to be adopted to simulate the amounts of erosion that lead to rill formation in the gravelly soil material under the dry climate in the study site. This suggests that the process that has led to rill formation is not included in the model. We suggest two possible processes. First, ~~the presence of groundwater~~permafrost that is present not far under the surface~~, which, when frozen,~~ can act as an impermeable layer. Combination of seeping groundwater and overland flow at ridge escarpments can then disaggregate coarse material and remove fine material (Higgins and Osterkamp, 1990). This seepage erosion occurs in cliffs and riverbanks (Fox et al., 2007; Higgins and Osterkamp, 1990), but has, to our knowledge, not been described for marine terrace sequences. Second, occasional heavy storms and high tides in the period soon after uplift above sea level may have caused temporary flooding of a beach trough that was already protected by a beach ridge. Drainage of the trough after a storm passes can have formed the rills. Both processes fit with the observed absence of a clear relation between rill size and age: the conditions that initiate rill erosion would be most prevalent after limited uplift over sea level.

Although these erosion rills occur in most of the terrace boundaries, most water is currently drained parallel to the ridges, towards the tundra lakes. These again drain to the Ebba river or the Petunia bay. Because the flow velocity through these lakes is very low, no erosion occurs.

The rate of aeolian deposition was estimated from observations without model simulations. However, a complicating factor is that this was based on present soil properties: the rate of aeolian deposition was based on current thickness of aeolian cover. Ultimately, part of the silt was translocated from the simulated aeolian deposits to deeper layers, resulting in an underestimation of thickness of ~~1A~~1AC horizons. This effect is visible for instance in the overestimation of gravel and underestimation of sand in the top parts of profiles in trough positions (Fig. 8).

The coefficient of determination of the regression between thickness of ~~1A~~1AC horizons and age (Section 4.3) shows that age only explains ~~a small part~~29% of ~~variation~~the variance in ~~1A~~1AC horizon thickness. This indicates that other factors such as the initial topography, wind ~~shadows~~shadow, hydrological properties, variation in surface cover by vegetation ~~cover~~ and bacterial soil crusts and reworking of aeolian sediments (e.g. Paluszkiewicz, 2003), which were not considered in our model, also play a -role.

The spatial heterogeneity of aeolian deposition is visible in shorter-term measurements in the study area. Deposition during the summer periods of 2012-2014 ranged from 3 to 1713 g m^{-2}

~~summer season~~[-1] ~~(Rymer, 2015)~~per summer season, depending on morphological position and vegetation cover (Rymer, 2015), while niveo-aeolian deposition in the years 2000-2005 ranged between 70 and 115 g m^{-2} ~~y~~a^{-1} (Rachlewicz, 2010). In comparison, aeolian deposition in Hornsund, southern Spitsbergen, was 300-400 g m^{-2} ~~y~~a^{-1} for the winter of 1957/58 (Czeppe and Jagielloński, 1966). The higher numbers in these measured ranges are about an order of magnitude larger than the average deposition rates found by our observation of aeolian horizon ~~observation (31~~thickness (40 g m^{-2} ~~y~~a^{-1}). Part of this difference can be caused by reworking of ~~short-term~~recent deposits ~~over time~~ by continued aeolian activity, another by our underestimation of the thickness of aeolian deposits by observing them after some of the silt has eluviated from them. On top of the spatial heterogeneity, there is also a large temporal variation in niveo-aeolian deposition rates (Christiansen, 1998).

5.3 Soil formation

Both physical and chemical weathering in the Arctic are driven by moisture availability (Hall et al., 2002). Consequently, ~~-~~weathering occurs at a faster rate in the wetter troughs of the terraces. This expected ~~spatial~~ variation in weathering between different morphological settings was observed in particle size distributions (Fig. 7), but not quantified in the model, due to data limitations. Next to that, also the ANOVA indicates the significant role of morphological position on gravel, sand and silt fraction. However, it should be noted that silt is also significantly influenced by ~~influx of~~ aeolian ~~deposits~~influx.

~~The weathering rate was calculated based on the gravel fraction of the subsurface horizons – not of the surface horizon. This was done in an attempt to exclude the effect of other processes on grain size changes. Nonetheless, dissolution (chemical weathering), which mainly reduces the silt fraction (Courty et al., 1994), may have affected grain sizes in the subsurface. Less fine material in the subsurface of older soils means more coarse material, which subsequently results in an underestimation of physical weathering rates. More, independent observations would be needed to disentangle the effects of physical and chemical weathering.~~

The physical weathering rate was calculated based on the gravel fraction of the subsurface horizons – not of the surface horizon. This was done in an attempt to exclude the effect of other processes on grain size changes. Nonetheless, chemical weathering in the form of dissolution may have affected the grain size distribution in the subsurface. Dissolution mainly affects the fine fraction, as it has a larger reactive surface area (Courty et al., 1994; Ford and Williams, 1989, p. 28). Less fine material in the subsurface means that the fraction of coarse material is higher. This subsequently results in an underestimation of the physical weathering rate, as this is based on the coarse fraction. Independent observations would be needed to disentangle the effects of physical and chemical weathering. For example, scanning electron microscope (SEM) could be used to identify surface morphologies related to certain weathering processes (e.g. Andò et al., 2012; Mavris et al., 2012). The mineralogical content of the groundwater, together with known temperatures, could provide constraints on dissolution rates (Dragon and Marciniak, 2010).

Consequently, the calculated weathering rate must be considered a combined physical and chemical weathering rate. This rate of ~~4.06~~1.01*10^{-5} kg kg^{-1} ~~y~~a^{-1} (~~4.06~~1.01*10^{-3} % ~~y~~a^{-1}) is orders of magnitudes lower than in field weathering experiments of the dominantly chemical weathering of granite and dolomite in Swedish Lapland (Dixon et al., 2001; Thorn et al., 2002). These resulted in a weight loss of 0.121 and 0.326 % ~~y~~a^{-1} respectively for an experiment of 5 years. Two reasons for this difference present themselves: time-decreasing weathering rates and moisture availability. Weathering rates decrease with time, amongst others due to precipitation of secondary minerals which slow the dissolution process ~~(Langman et al., 2015). These secondary minerals were~~(Langman et al., 2015; White et al., 1996). These secondary minerals were widely observed in Ebba valley, partially coating gravel (c.f. Courty et al., 1994). It is also likely that long term weathering rates in Swedish Lapland exceed those found in the Ebba valley because of the much larger precipitation ~~(1750 mm y^{-1}, Dixon et al., 2001)~~. Other weathering studies also indicate the dominant control of moisture in determining both physical and chemical weathering rates (e.g. Egli et al., 2015; Hall et al., 2002; Langston et al., 2011; Matsuoka, 1990; Wu, 2016; Yokoyama and Matsukura, 2006).

It can nonetheless be argued that dissolution is a significant process in our marine terraces. This is also apparent in the field observations. 2A horizons have a lower $CaCO_3$ content than 2B, 2B*l* and 2BC horizons. This is consistent with observations elsewhere in Spitsbergen of a more active dissolution regime in near surface horizons, compared to subsurface horizons (Courty et al., 1994; Forman and Miller, 1984). Dissolution mainly occurs in the fine soil mass due to its larger reactive surface. Consequently, the fine fraction in ~~1A~~1AC and 2A horizons consists of less CaCO3.

Dissolution was not included in model simulations. This should have caused overestimation of fine material in the model output. However, model results instead show lower sand and silt contents than observed (Fig. 7, Fig. 8, Table 4). For trough positions, this is partly due to underestimation of the thickness of ~~1A~~1AC horizons (see above). By this underestimation, the thinner ~~1A~~1AC horizons give way to underlying marine deposits in the model outputs. Their higher gravel content distorts the comparison between observed and simulated profiles, leading to an underestimation of sand content and fraction. Silt properties are not influenced by this error, as the eluviation rate was calibrated using valley positions. As a consequence, silt predictions there show a low error.

This disturbance by a wrongly estimated thickness of the aeolian cover is not present in ridge positions. However, also for those positions sand and silt contents are underestimated. Simulated silt content shows the largest deviation from field observations (Fig. 8, Table 4). This indicates that there is another source of sand and silt in ridge positions.

One source of silt is in situ weathering of coarse material into finer material (Fahey and Dagesse, 1984; Forman and Miller, 1984). ~~Another source is an ex situ one, namely aeolian deposition.~~Another source is an ex situ one, namely aeolian deposition (e.g. Locke, 1986). This is observed in trough positions, which display a higher silt fraction throughout the whole profile, compared to ridge positions (Fig. 7). The heterogeneous deposition of aeolian material over trough positions on the area has resulted in ~~an even~~a heterogeneous silt source for the subsurface. Hence, the ANOVA shows no significant relation between ~~age~~terrace level and silt fraction.

Deposition occurs partly through entrapment with falling snow (Rachlewicz, 2010). Meltwater from this snow partly infiltrates in the permeable gravelly soils. This downward flow of water can transport part of the silt it had captured, increasing the silt fraction in the subsurface. This process can also act as a source of silt in ridge positions. Material left behind on the surface can be reworked by strong summer winds, leaving no trace of aeolian deposits on these positions. This theory contradicts the observations of Forman and Miller (1984), who claim that silt in their studied marine ridges on western Spitsbergen mainly originates from in situ frost weathering and dissolution. They attribute this to absence of a major source area, absence of silt on the surface and absence of vegetation to entrap sediments. In the Ebba valley, the proglacial sandur plain acts as a major sediment source. Next to that, our observations of 2A horizons, which partly reach the surface, show high amounts of silt compared to lower lying horizons (Table 3). Due to these different conditions in the Ebba valley, it is possible that ridge positions also profit from aeolian silt input. This also can explain the deficit of silt in model simulations (Fig. 7).

The enrichment of silt from aeolian material, silt caps located on top of clasts and heterogeneous distribution of silt in the 2B*l* horizons suggest that eluviation is responsible for the silt redistribution, instead of frost sorting, as suggested by Bockheim and Tarnocai (1998). Addition of a depth decay function in the simulation of silt translocation proved to result in simulated profiles comparable to the observed profiles (Fig. 7). This decay in eluviation rate with depth represents the limited water flux in the subsurface. Due to a shallow unfrozen soil in the snow melt season, the water cannot reach deeply into the soil and starts to flow laterally. Later in the season, when the active layer is thawed, the water flux is limited, because precipitation is very limited. More detailed descriptions of the silt content throughout the whole profile can help to better understand the silt dynamics in these Arctic environments.

5.4 Temporal and spatial soil-landscape interactions

The variation in simulated soil profiles is smaller than the variation in observed soil profiles (Fig. 7). We presume that this is due to a variation in boundary conditions that is not captured in the model. Particularly, in reality, the grain size distribution of the original parent material will differ between locations, and aeolian deposition rates vary both in space and time. Next to that, temporal variation in climate is not considered. The glacial retreat since the beginning of the Holocene indicates the general warming climate in Svalbard, which also includes several colder episodes (e.g. Svendsen and Mangerud, 1997b)~~.~~(Svendsen and Mangerud, 1997a). The effects of these changing temperatures on process rates such as weathering rates were not included in the model. Precipitation and evaporation rates were also not constant during the Holocene. Courty et al. (1994) show that characteristics of secondary carbonates on subsurface clasts indicate different climatic and biogenic episodes. Although their research was conducted on western Spitsbergen which has a much wetter climate than central Spitsbergen, it is likely that ~~such~~ variations in climate occurred over the complete Svalbard archipelago.

The elevation differences between ridges and troughs in the study area are the main driving force for spatial soil heterogeneity. Water flow accumulates in the relatively sheltered trough positions. Consequently, weathering occurs at a faster rate and there is a ~~bit more plant growth.~~higher vegetation density. These plants capture a part of the aeolian sediment that has been deposited with freshly fallen snow. The resulting ~~1A~~1AC horizon, consisting of finer material, holds more water than the marine sediments, resulting in more plant growth. This feedback has resulted in a local aeolian ~~covers of~~cover up to 70 cm. Note that this process is not expected to continue over longer timescales, because the aeolian sediments will ultimately grow out of their sheltered and, more importantly, humid positions, becoming susceptible to reworking by wind erosion.

Ultimately, Arctic soil development is not as straightforward as we hypothesized in the beginning of this paper. The interplay between different processes, known and unknown, together with variations in initial and boundary conditions in soil and landscape development has resulted in a complex soil-landscape system. Additional research ~~is~~would be required to further unravel soil and landscape development in this fragile environment, especially in the context of a changing climate.

6 Conclusions

This study combined different methods to study soil development on a series of marine terraces in Central Spitsbergen. The analysis of the ~~combined~~ results ~~of these methods~~ led to the following conclusions:

- The changes in soil properties of the gravelly soils on the marine terraces ~~display clear effects of~~ can be attributed to different soil forming processes, such as physical (frost action) and chemical weathering (dissolution) and translocation of silt. Dissolution mainly occurs in A horizons developed in marine material. Translocation of silt occurs everywhere in the landscape, following the water flow.
- Optically Stimulated Luminescence ~~dating~~ (OSL) ~~appears a good method for dating isostatic uplift rates of the marine terraces. Its~~ results ~~confirm~~support earlier radiocarbon dates from the area. Moreover, an uplift curve constructed based on both types of dates concurs with a nearby uplift curve, indicating the potential of OSL for measuring uplift rates in this setting. Combining these datings with field observations enabled the calculation of process rates using field observations.
- However, determining historical rates of weathering and aeolian deposition using current soil properties is difficult when multiple processes have influenced those properties. Especially dissolution, which removes material from the soil, distorts the mass balance of soil constituents that was used to calculate rates.
- Simulation of soil development in a landscape context with soilscape evolution model LORICA was successful in terms of simulating trends in soil properties. However, there were significant discrepancies between field observations and model results. The larger variation in field observations than in model simulations is likely ~~mainly~~ due to spatially and temporally varying boundary conditions that were not included in simulations. More importantly, bias in model outcomes helped to increase our understanding of Arctic soil development in the marine terraces.
- Soil development is heavily influenced by geomorphic processes, mainly aeolian deposition. Deposition acts as a source of fine material, which mainly accumulates in relatively sheltered beach trough positions. However, our results are consistent with suggestions that aeolian silt has also been added to soils in beach ridge positions.

Erosion of overland flow plays a minor role, compared to erosion by extruding groundwater or by the effects of storms on young terraces.

7 Author contribution

This paper is based on the master ~~thesis research~~theses of W.M. van der Meij and C.M.F.J.J. de Kleijn, under supervision of A.J.A.M. Temme and G.B.M. Heuvelink. Fieldwork was performed by W.M. van der Meij and C.M.F.J.J. de Kleijn at the Adam Mickiewicz University Polar Station (AMUPS), facilitated by Z. Zwoliński and G. Rachlewicz. Fieldwork was supported by K. Rymer. T. Reimann performed the OSL analysis. W.M. van der Meij and A.J.A.M. Temme adjusted the model code and W.M. van der Meij performed the simulations. M. Sommer provided conceptual pedological context and funding for the first author to work on the paper. The manuscript has been prepared by the first three authors with contributions from all other authors.

8 Acknowledgements

W.M van der Meij, A.J.A.M. Temme and C.~~N~~M.F.J.J. de Kleijn are grateful to the colleagues of the Adam Mickiewicz University for the opportunity of performing fieldwork at their Arctic research station. We acknowledge dr. Bart Makaske for fruitful discussions about beach morphology nomenclature. G. Rachlewicz and K. Rymer were supported by Polish National Science Centre grant no. 2011/03/B/ST10/06172.

9 References

Aitken, M. J.: An introduction to optical dating: the dating of Quaternary sediments by the use of photon-stimulated luminescence, Oxford University Press, 1998.

Andò, S., Garzanti, E., Padoan, M., and Limonta, M.: Corrosion of heavy minerals during weathering and diagenesis: A catalog for optical analysis, Sedimentary Geology, 280, 165-178, 2012.

Arctic Climate Impact Assessment: Impacts of a Warming Arctic - Arctic Climate Impact Assessment, Cambridge University Press, Cambridge, UK, 2004.

Ballantyne, C. K.: Paraglacial geomorphology, Quaternary Science Reviews, 21, 1935-2017, 2002.

Ballarini, M., Wallinga, J., Murray, A., Van Heteren, S., Oost, A., Bos, A., and Van Eijk, C.: Optical dating of young coastal dunes on a decadal time scale, Quaternary Science Reviews, 22, 1011-1017, 2003.

Birkeland, P.: Quaternary soil chronosequences in various environments – extremely arid to humid tropical. In: Weathering, Soils & Paleosols, Edited by: Martini, I. P. and Chesworth, W., Elsevier, Amsterdam, 261-281, 1992.

Birkeland, P. W.: Soil-geomorphic research—a selective overview, Geomorphology, 3, 207-224, 1990.

Bockheim, J. and Tarnocai, C.: Recognition of cryoturbation for classifying permafrost-affected soils, Geoderma, 81, 281-293, 1998.

Bockheim, J. G. and Ugolini, F. C.: A review of pedogenic zonation in well-drained soils of the southern circumpolar region, Quaternary Research, 34, 47-66, 1990.

Briant, R. M. and Bateman, M. D.: Luminescence dating indicates radiocarbon age underestimation in late Pleistocene fluvial deposits from eastern England, Journal of Quaternary Science, 24, 916-927, 2009.

Buchwal, A., Rachlewicz, G., Fonti, P., Cherubini, P., and Gärtner, H.: Temperature modulates intra-plant growth of Salix polaris from a high Arctic site (Svalbard), Polar Biology, 36, 1305-1318, 2013.

Burns, S. F.: Alpine soil distribution and development, Indian Peaks, Colorado Front Range, PhD dissertation, University of Colorado at Boulder, 360 pp., 1980.

Christiansen, H. H.: 'Little Ice Age' nivation activity in northeast Greenland, The Holocene, 8, 719-728, 1998.

Courty, M. A., Marlin, C., Dever, L., Tremblay, P., and Vachier, P.: The properties, genesis and environmental significance of calcitic pendents from the High Arctic (Spitsbergen), Geoderma, 61, 71-102, 1994.

Cunningham, A. C. and Wallinga, J.: Selection of integration time intervals for quartz OSL decay curves, Quaternary Geochronology, 5, 657-666, 2010.

Czeppe, Z. and Jagielloński, U.: Przebieg głównych procesów morfogenetycznych w południowo-zachodnim Spitsbergenie, Uniwersytet Jagielloński, 1966.

Dixon, J. C., Thorn, C. E., Darmody, R. G., and Schlyter, P.: Weathering rates of fine pebbles at the soil surface in Kärkevagge, Swedish Lapland, Catena, 45, 273-286, 2001.

Dragon, K. and Marciniak, M.: Chemical composition of groundwater and surface water in the Arctic environment (Petuniabukta region, central Spitsbergen), Journal of Hydrology, 386, 160-172, 2010.

Egli, M., Dahms, D., and Norton, K.: Soil formation rates on silicate parent material in alpine environments: Different approaches-different results?, Geoderma, 213, 320-333, 2014.

Egli, M., Lessovaia, S. N., Chistyakov, K., Inozemzev, S., Polekhovsky, Y., and Ganyushkin, D.: Microclimate affects soil chemical and mineralogical properties of cold alpine soils of the Altai Mountains (Russia), Journal of Soils and Sediments, 15, 1420-1436, 2015.

Egli, M., Wernli, M., Kneisel, C., and Haeberli, W.: Melting glaciers and soil development in the proglacial area Morteratsch (Swiss Alps): I. Soil type chronosequence, Arctic, Antarctic, and Alpine Research, 38, 499-509, 2006.

Elster, J. and Rachlewicz, G.: Petuniabukta, Billefjorden in Svalbard: Czech-Polish long term ecological and geographical research, Polish Polar Research, 33, 289-295, 2012.

Fahey, B. D. and Dagesse, D. F.: An experimental study of the effect of humidity and temperature variations on the granular disintegration of argillaceous carbonate rocks in cold climates, Arctic and Alpine Research, 1984. 291-298, 1984.

FAO: Guidelines for soil description, Rome, 2006.

Fischer, Z.: The influence of humidity and temperature upon the rate of soil metabolism in the area of Hornsund (Spitsbergen), Pol. Polar Res, 11, 17-24, 1990.

Ford, D. C. and Williams, P. W.: Karst geomorphology and hydrology, John Wiley and Sons, Chichester, 1989.

Forland, E. J., Benestad, R., Hanssen-Bauer, I., Haugen, J. E., and Skaugen, T. E.: Temperature and Precipitation Development at Svalbard 1900-2100, Advances in Meteorology, 2011, 14 pages, http://dx.doi.org/10.1155/2011/893790, 2011.

Forman, S. L., Lubinski, D. J., Ingólfsson, Ó., Zeeberg, J. J., Snyder, J. A., Siegert, M. J., and Matishov, G. G.: A review of postglacial emergence on Svalbard, Franz Josef Land and Novaya Zemlya, northern Eurasia, Quaternary Science Reviews, 23, 1391-1434, 2004.

Forman, S. L. and Miller, G. H.: Time-dependent soil morphologies and pedogenic processes on raised beaches, Broggerhalvoya, Spitsbergen, Svalbard archipelago, Arctic & Alpine Research, 16, 381-394, 1984.

Forman, S. L. and Polyak, L.: Radiocarbon content of pre-bomb marine mollusks and variations in the reservoir age for coastal areas of, Geophysical Research Letters, 24, 885-888, 1997.

Fox, G. A., Wilson, G. V., Simon, A., Langendoen, E. J., Akay, O., and Fuchs, J. W.: Measuring streambank erosion due to ground water seepage: correlation to bank pore water pressure, precipitation and stream stage, Earth Surface Processes and Landforms, 32, 1558-1573, 2007.

Galbraith, R. F., Roberts, R. G., Laslett, G., Yoshida, H., and Olley, J. M.: Optical dating of single and multiple grains of quartz from Jinmium rock shelter, northern Australia: part I, experimental design and statistical models, Archaeometry, 41, 339-364, 1999.

Gibas, J., Rachlewicz, G., and Szczuciński, W.: Application of DC resistivity soundings and geomorphological surveys in studies of modern Arctic glacier marginal zones, Petuniabukta, Spitsbergen, Polish Polar Research, 26, 239-258, 2005.

Gulińska, J., Rachlewicz, G., Szczuciński, W., Barałkiewicz, D., Kózka, M., Bulska, E., and Burzyk, M.: Soil contamination in high arctic areas of human impact, central Spitsbergen, Svalbard, Polish Journal of Environmental Studies, 12, 701-707, 2003.

Hall, K., Thorn, C. E., Matsuoka, N., and Prick, A.: Weathering in cold regions: some thoughts and perspectives, Progress in Physical Geography, 26, 577-603, 2002.

Higgins, C. G. and Osterkamp, W. R.: Seepage-induced cliff recession and regional denudation. In: Groundwater Geomorphology: The Role of Subsurface Water in Earth-Surface Processes and Landforms, , Edited by: Higgins, C. G. and Coates, D. R., Geol. Soc. Am. Spec. Pap, Boulder, Colorado, 291-318, 1990.

Hodkinson, I. D., Coulson, S. J., and Webb, N. R.: Community assembly along proglacial chronosequences in the high Arctic: vegetation and soil development in north-west Svalbard, Journal of Ecology, 91, 651-663, 2003.

IUSS Working Group WRB: World Reference Base for Soil Resources 2014, update 2015 International soil classification system for naming soils and creating legends for soil maps, FAO, Rome, 192 pp., 2015.

IUSS Working Group WRB: World Reference Base for Soil Resources 2014. International soil classification system for naming soils and creating legends for soil maps, FAO, Rome, 191 pp., 2014.

Janssen, P. and Heuberger, P.: Calibration of process-oriented models, Ecological Modelling, 83, 55-66, 1995.

Jónsdóttir, I. S., Austrheim, G., and Elvebakk, A.: Exploring plant-ecological patterns at different spatial scales on Svalbard UNIS, Longyearbyen82-481-0008-1 (ISBN), 87 pp., 2006.

Kabala, C. and Zapart, J.: Initial soil development and carbon accumulation on moraines of the rapidly retreating Werenskiold Glacier, SW Spitsbergen, Svalbard archipelago, Geoderma, 175, 9-20, 2012.

Kabala, C. and Zapart, J.: Recent, relic and buried soils in the forefield of Werenskiold Glacier, SW Spitsbergen, Polish Polar Research, 30, 161-178, 2009.

Kłysz, P., Lindner, L., Makowska, A., Marks, L., and Wysokiński, L.: Late Quaternary glacial episodes and sea level changes in the northeastern Billefjorden region, Central Spitsbergen, Acta Geologica Polonica, 38, 107-123, 1988.

Kłysz, P., Lindner, L., Marks, L., and Wysokiński, L.: Late Pleistocene and Holocene relief remodelling in the Ebbadalen-Nordenskióldbreen region in Olav V Land, central Spitsbergen, Polish Polar Research, 10, 277-301, 1989.

Köppen, W. P.: Grundriss der Klimakunde, Walter de Gruyter, Berlin, 1931.

Langman, J. B., Blowes, D. W., Sinclair, S. A., Krentz, A., Amos, R. T., Smith, L. J., Pham, H. N., Sego, D. C., and Smith, L.: Early evolution of weathering and sulfide depletion of a low-sulfur, granitic, waste rock in an Arctic climate: A laboratory and field site comparison, Journal of Geochemical Exploration, 2015. 2015.

Langston, A. L., Tucker, G. E., Anderson, R. S., and Anderson, S. P.: Exploring links between vadose zone hydrology and chemical weathering in the Boulder Creek critical zone observatory, Applied Geochemistry, 26, S70-S71, 2011.

Láska, K., Witoszová, D., and Prošek, P.: Weather patterns of the coastal zone of Petuniabukta, central Spitsbergen in the period 2008-2010, Polish Polar Research, 33, 297-318, 2012.

Lindner, L. and Marks, L.: Geodynamic aspects of studies of Quaternary inland sediments in South Spitsbergen (attempt to synthesis), Pol. Polar Res, 11, 365-387, 1990.

Locke, W. W.: Fine particle translocation in soils developed on glacial deposits, southern Baffin Island, NWT, Canada, Arctic and Alpine Research, 1986. 33-43, 1986.

Long, A. J., Strzelecki, M. C., Lloyd, J. M., and Bryant, C. L.: Dating High Arctic Holocene relative sea level changes using juvenile articulated marine shells in raised beaches, Quaternary Science Reviews, 48, 61-66, 2012.

Madsen, A. T., Murray, A., Andersen, T., Pejrup, M., and Breuning-Madsen, H.: Optically stimulated luminescence dating of young estuarine sediments: a comparison with 210 Pb and 137 Cs dating, Marine Geology, 214, 251-268, 2005.

Makaske, B. and Augustinus, P. G.: Morphologic changes of a micro-tidal, low wave energy beach face during a spring-neap tide cycle, Rhone-Delta, France, Journal of Coastal Research, 1998. 632-645, 1998.

Mann, D., Sletten, R., and Ugolini, F.: Soil development at Kongsfjorden, Spitsbergen, Polar Research, 4, 1-16, 1986.

Matsuoka, N.: Mechanisms of rock breakdown by frost action: an experimental approach, Cold Regions Science and Technology, 17, 253-270, 1990.

Mavris, C., Götze, J., Plötze, M., and Egli, M.: Weathering and mineralogical evolution in a high Alpine soil chronosequence: A combined approach using SEM–EDX, cathodoluminescence and Nomarski DIC microscopy, Sedimentary Geology, 280, 108-118, 2012.

Mazurek, M., Paluszkiewicz, R., Rachlewicz, G., and Zwoliński, Z.: Variability of water chemistry in tundra lakes, Petuniabukta coast, Central Spitsbergen, Svalbard, The Scientific World Journal, 2012, 2012.

McBratney, A. B., Minasny, B., Cattle, S. R., and Vervoort, R. W.: From pedotransfer functions to soil inference systems, Geoderma, 109, 41-73, 2002.

Mejdahl, V.: Thermoluminescence dating: Beta-dose attenuation in quartz grains, Archaeometry, 21, 61-72, 1979.

Melke, J.: Characteristics of soil filamentous fungi communities isolated from various micro−relief forms in the high Arctic tundra (Bellsund region, Spitsbergen), Polish Polar Research, 28, 57-73, 2007.

Melke, J. and Chodorowski, J.: Formation of arctic soils in Chamberlindalen, Bellsund, Spitsbergen, Polish Polar Research, 27, 119-132, 2006.

Murray, A. S. and Wintle, A. G.: The single aliquot regenerative dose protocol: potential for improvements in reliability, Radiation Measurements, 37, 377-381, 2003.

Paluszkiewicz, R.: Zróżnicowanie natężenia transportu eolicznego w warunkach polarnych jako efekt zmienności czynników meteorologicznych na przykładzie doliny Ebby (Petuniabukta, Billefjorden, Spitsbergen Środkowy) [Differentiation of eolitic transport intensity in polar conditions as an effect of variability in meteorological factors. Case study of the Ebba valley]. In: The Functioning of Polar Ecosystems as Viewed Against global Environmental Changes, Edited by: Olech, M. A., XXIX International Polar Symposium, Kraków, 19-21 September 2003, 235-238, 2003.

Pereverzev, V. N.: Soils developed from marine and moraine Deposits on the Billefjord coast, West Spitsbergen, Eurasian Soil Science, 45, 1023-1032, 2012.

Pereverzev, V. N. and Litvinova, T. I.: Soils of sea terraces and bedrock slopes of fiords in Western Spitsbergen, Eurasian Soil Science, 43, 239-247, 2010.

Péwé, T. L., Rowan, D. E., Péwé, R. H., and Stuckenrath, R.: Glacial and Periglacial geology of northwest Blomesletta peninsula, Spitsbergen, Svalbard, Norsk Polarinsititut Skrifter, 177, 32pp, 1982.

Phillips, J. D.: The robustness of chronosequences, Ecological Modelling, 298, 16-23, 2015.

Ping, C.-L., Michaelson, G. J., Jorgenson, M. T., Kimble, J. M., Epstein, H., Romanovsky, V. E., and Walker, D. A.: High stocks of soil organic carbon in the North American Arctic region, Nature Geoscience, 1, 615-619, 2008.

Prach, K., Klimešová, J., Košnar, J., Redčenko, O., and Hais, M.: Variability of contemporary vegetation around Petuniabukta, central Spitsbergen, Polish Polar Research, 33, 383-394, 2012.

Prescott, J. R. and Hutton, J. T.: Cosmic ray contributions to dose rates for luminescence and ESR dating: large depths and long-term time variations, Radiation measurements, 23, 497-500, 1994.

Preusser, F., Degering, D., Fuchs, M., Hilgers, A., Kadereit, A., Klasen, N., Krbetschek, M., Richter, D., and Spencer, J. Q.: Luminescence dating: basics, methods and applications, Quaternary Science Journal, 57, 95-149, 2008.

Przybylak, R., Araźny, A., Nordli, Ø., Finkelnburg, R., Kejna, M., Budzik, T., Migała, K., Sikora, S., Puczko, D., Rymer, K., and Rachlewicz, G.: Spatial distribution of air temperature on Svalbard during 1 year with campaign measurements, International Journal of Climatology, 34, 3702-3719, 2014.

Rachlewicz, G.: Contemporary Sediment Fluxes and Relief Changes in High Artic Glacierized Valley Systems (Billefjorden, Central Spitsbergen), Wydawnictwo Naukowe Uniwersytetu im. Adama Mickiewicza, Poznań, 2009.

Rachlewicz, G.: Paraglacial modifications of glacial sediments over millennial to decadal time-scales in the high arctic (Billefjorden, central Spitsbergen, Svalbard), Quaestiones Geographicae, 29, 59-67, 2010.

Rachlewicz, G. and Szczuciński, W.: Changes in thermal structure of permafrost active layer in a dry polar climate, Petuniabukta, Svalbard, Polish Polar Research, 29, 261-278, 2008.

Rachlewicz, G., Zwoliński, Z., Kostrzewski, A., and Birkenmajer, K.: Geographical environment in the vicinity of the Adam Mickiewicz University in Poznań Polar Station–Petuniabukta. In: Ancient and Modern Geoecosystems of Spitsbergen. Polish geomorphological research, Edited by: Zwoliński, Z., Kostrzewski, A., and Pulina, M., Bogucki Wydawnictwo Naukowe, Poznań, 205-243, 2013.

Reimann, T., Lindhorst, S., Thomsen, K. J., Murray, A. S., and Frechen, M.: OSL dating of mixed coastal sediment (Sylt, German Bight, North Sea), Quaternary Geochronology, 11, 52-67, 2012.

Reimann, T., Naumann, M., Tsukamoto, S., and Frechen, M.: Luminescence dating of coastal sediments from the Baltic Sea coastal barrier-spit Darss–Zingst, NE Germany, Geomorphology, 122, 264-273, 2010.

Reimer, P. J., Bard, E., Bayliss, A., Beck, J. W., Blackwell, P. G., Ramsey, C. B., Buck, C. E., Cheng, H., Edwards, R. L., and Friedrich, M.: IntCal13 and Marine13 radiocarbon age calibration curves 0–50,000 years cal BP, Radiocarbon, 55, 1869-1887, 2013.

Rodnight, H., Duller, G., Wintle, A., and Tooth, S.: Assessing the reproducibility and accuracy of optical dating of fluvial deposits, Quaternary Geochronology, 1, 109-120, 2006.

Rymer, K.: The aeolian processes observations in Ebba valley (central Spitsbergen), 2010-2015 (Conference abstract), available at: http://www.polarknow.us.edu.pl/IPSiS/pdf/Pe_20.pdf, (last access: 14 October 2015), 2015.

Salvigsen, O.: Occurrence of pumice on raised beaches and Holocene shoreline displacement in the inner Isfjorden area, Svalbard, Polar Research, 2, 107-113, 1984.

Sauer, D., Finke, P., Sørensen, R., Sperstad, R., Schülli-Maurer, I., Høeg, H., and Stahr, K.: Testing a soil development model against southern Norway soil chronosequences, Quaternary International, 265, 18-31, 2012.

Scheffers, A., Engel, M., Scheffers, S., Squire, P., and Kelletat, D.: Beach ridge systems - archives for holocene coastal events?, Progress in Physical Geography, 36, 5-37, 2012.

Sevink, J., Koster, E., van Geel, B., and Wallinga, J.: Drift sands, lakes, and soils: the multiphase Holocene history of the Laarder Wasmeren area near Hilversum, the Netherlands, Netherlands Journal of Geosciences, 92, 243-266, 2013.

Slaymaker, O.: Criteria to distinguish between periglacial, proglacial and paraglacial environments, Quaestiones Geographicae, 30, 85-94, 2011.

Sommer, M. and Schlichting, E.: Archetypes of catenas in respect to matter—a concept for structuring and grouping catenas, Geoderma, 76, 1-33, 1997.

Strzelecki, M. C.: High Arctic Paraglacial Coastal Evolution in Northern Billefjorden, Svalbard, Ph.D., Department of Geography, Durham University, Durham, 303 pp., 2012.

Stuiver, M. and Reimer, P. J.: Extended 14C data base and revised CALIB 3.0 14 C age calibration program, Radiocarbon, 35, 215-230, 1993.

Svendsen, J. I. and Mangerud, J.: Holocene glacial and climatic variations on Spitsbergen, Svalbard, The Holocene, 7, 45-57, 1997a.

Svendsen, J. I. and Mangerud, J.: Holocene glacial and climatic variations on Spitsbergen, Svalbard, Holocene, 7, 45-57, 1997b.

Temme, A. J. A. M. and Lange, K.: Pro-glacial soil variability and geomorphic activity - the case of three Swiss valleys, Article in press, 2014. 2014.

Temme, A. J. A. M. and Vanwalleghem, T.: LORICA – A new model for linking landscape and soil profile evolution: development and sensitivity analysis, Computers & Geosciences, 2015. http://dx.doi.org/10.1016/j.cageo.2015.1008.1004, 2015.

Thorn, C. E., Darmody, R. G., Dixon, J. C., and Schlyter, P.: Weathering rates of buried machine-polished rock disks, Kärkevagge, Swedish Lapland, Earth Surface Processes and Landforms, 27, 831-845, 2002.

Ugolini, F. C.: Pedogenic zonation in the well-drained soils of the arctic regions, Quaternary Research, 26, 100-120, 1986.

Ugolini, F. C., Corti, G., and Certini, G.: Pedogenesis in the sorted patterned ground of Devon plateau, Devon Island, Nunavut, Canada, Geoderma, 136, 87-106, 2006.

Vreeken, W. v.: Principal kinds of chronosequences and their significance in soil history, Journal of Soil Science, 26, 378-394, 1975.

Walker, M.: Quaternary Dating Methods, John Wiley and Sons, Chichester, 2005.

White, A. F., Blum, A. E., Schulz, M. S., Bullen, T. D., Harden, J. W., and Peterson, M. L.: Chemical weathering rates of a soil chronosequence on granitic alluvium: I. Quantification of mineralogical and surface area changes and calculation of primary silicate reaction rates, Geochimica et Cosmochimica Acta, 60, 2533-2550, 1996.

Wu, W.: Hydrochemistry of inland rivers in the north Tibetan Plateau: Constraints and weathering rate estimation, Science of The Total Environment, 541, 468-482, 2016.

Yokoyama, T. and Matsukura, Y.: Field and laboratory experiments on weathering rates of granodiorite: separation of chemical and physical processes, Geology, 34, 809-812, 2006.

Zwoliński, Z., Gizejewski, J., Karczewski, A., Kasprzak, M., Lankauf, K. R., Migon, P., Pekala, K., Repelewska-Pekalowa, J., Rachlewicz, G., Sobota, I., Stankowski, W., and Zagorski, P.: Geomorphological settings of Polish research stations on Spitsbergen, Landform Analysis, 22, 125-143, 2013.

Zwoliński, Z., Kostrzewski, A., and Rachlewicz, G.: Environmental changes in the Arctic. In: Environmental Changes and Geomorphic Hazards Edited by: Singh, S., Starkel, L., and Syiemlieh, H. J., Bookwell, Delhi, 23-36, 2008.

10 Tables

Table 1: Settings and parameters used as input for the LORICA model

General		Simulation time (~~y~~a)		~~14393~~13300
		Timestep (~~y~~a)		1
		Number of soil layers		10
		Initial soil depth (m)		1.5
		Precipitation (m ~~y~~a^{-1})		0.2
		Evaporation (m ~~y~~a^{-1})		0.075
		Infiltration (m ~~y~~a^{-1})		0.075
		Initial composition of the soil	Gravel (%)	~~90~~95
			Sand (%)	~~10~~5
			Silt (%)	0
Geomorphic processes	Water erosion and deposition	p (multiple flow factor)		2
		m (exponent of overland flow)		1.67
		n (exponent of slope)		1.3
		K (erodibility)		0.0003
		Erosion threshold		0.01
		Rock protection constant		1
		Bio protection constant		0.5
		Selectivity change constant		0
	Aeolian deposition	Maximum eluviation (kg a^{-1})		0.15
		Depth decay constant (m^{-1})		5
Soil forming processes	Physical weathering	Weathering rate constant (~~y~~a^{-1})		1.~~26~~01*10^{-5}
		Depth decay constant (m^{-1})		-~~2.22~~1.63
		Particle size constant (m)		5
		Particle size	Coarse fraction (m)	0.01
			Sand fraction (m)	0.002
			Silt fraction (m)	0.000065
	Silt translocation	Maximum eluviation (kg)		0.15
		Depth decay constant (m^{-1})		6
		Saturation constant		1

Table 2: OSL ages with uncertainty of 1σ for 3 samples taken in the study area (Fig. 1).

Location Fig. 1	NCL lab. code	Altitude (m)	Depth (m)	Palaeodose (Gy)	Dose rate (Gy/ka)	OSL age (ka)	Systematic error (ka)	Random error (ka)
I	NCL-2114067	5.5	0.57	5.9 ± 0.2	1.34 ± 0.05	4.4 ± 0.2	0.14	0.18
II	NCL-2114068	11.1	0.27	11.8 ± 0.6	1.62 ± 0.05	7.3 ± 0.4	0.23	0.37
III	NCL-2114066	41.6	0.57	20.3 ± 1.6	1.58 ± 0.05	12.8 ± 1.1	0.41	0.97

Experimental details are provided in Sect. 3.1.

Table 3: Average and standard deviation ~~of~~(between brackets) of soil properties of sampled horizons. Horizons with errors in sampling were left out. ~~The n indicates~~Counts indicate the ~~remaining~~amount of observed horizons, the total amount of samples~~.~~ can deviate from these numbers (cf. Fig. 5).The age ranges of the individual horizons were derived from the minimum and maximum altitude per terrace level and their relation with age (Fig. 3). Carbonate content was ~~measured~~estimated in the field according to FAO (2006).

Terrace level	Age range (a)	Horizon	Count	Thickness (m)	Gravel fraction (-)	Sand fraction (-)	Silt fraction (-)	OM fraction (-)	Bulk density (g cm-3)	CaCO3 (%)
1	1580 - 5675	1AC	2	0.12 (0.04)	0 (0)	0.88 (0.01)	0.12 (0.01)	0.06 (0.01)		2 - 10
		2A	2	0.12 (0.04)	0.18 (0.17)	0.63 (0.2)	0.19 (0.03)	0.07 (0.03)	0.93	2 - 10
		2B	0							
		2Bl	1	0.12	0.78	0.16	0.05	0.01		>25
		2BC	2	0.35 (0.07)	0.92 (0.03)	0.06 (0.04)	0.02 (0)	0 (0)	1.12	>25
2	4562 - 7041	1AC	4	0.12 (0.02)	0 (0)	0.84 (0.03)	0.15 (0.03)	0.06 (0)	1.21 (0.16)	2 – 10
		2A	3	0.1 (0.02)	0.42 (0.26)	0.47 (0.24)	0.11 (0.03)	0.02 (0.01)	1.32 (0.16)	>25
		2B	1	0.2	0.96	0.03	0.02	0	1.29	>25
		2Bl	6	0.38 (0.27)	0.82 (0.11)	0.14 (0.09)	0.04 (0.03)	0.01 (0.01)	1.31 (0.07)	>25
		2BC	6	0.42 (0.17)	0.86 (0.16)	0.12 (0.15)	0.02 (0.01)	0 (0)	1.34 (0.01)	>25
3	5092 - 8838	1AC	2	0.26 (0.08)	0 (0.01)	0.89 (0.01)	0.1 (0)	0.04 (0.01)	1.02 (0.43)	0 – 10
		2A	3	0.18 (0.1)	0.15 (0.1)	0.63 (0.05)	0.22 (0.09)	0.06 (0.05)	1.11 (0.37)	>25
		2B	1	0.23	0.52	0.44	0.04	0	1.5	>25
		2Bl	2	0.18 (0.11)	0.56 (0.16)	0.39 (0.16)	0.05 (0.01)	0.01 (0)	1.46 (0.1)	>25
		2BC	3	0.34 (0.07)	0.68	0.3	0.02	0		>25
4	7708 - 12662	1AC	9	0.3 (0.22)	0.02 (0.03)	0.91 (0.03)	0.08 (0.03)	0.03 (0.01)	1.37 (0.09)	0 – 10
		2A	5	0.17 (0.1)	0.17 (0.33)	0.69 (0.29)	0.14 (0.07)	0.04 (0.02)	1.3 (0.11)	0 - >25
		2B	0							
		2Bl	9	0.38 (0.24)	0.61 (0.12)	0.3 (0.09)	0.09 (0.04)	0.02 (0.01)	1.5 (0.15)	10 - >25
		2BC	7	0.29 (0.27)	0.68 (0.28)	0.3 (0.27)	0.02 (0.01)	0 (0)	1.56 (0.09)	10 - >25
5	10784 - 13535	1AC	6	0.28 (0.11)	0.01 (0.03)	0.91 (0.02)	0.08 (0.02)	0.03 (0.01)	1.37 (0.04)	2 – 10
		2A	4	0.2 (0.11)	0.4 (0.32)	0.51 (0.3)	0.09 (0.03)	0.03 (0.02)	1.34 (0.08)	0 - >25
		2B	2	0.34 (0.06)	0.67 (0.12)	0.27 (0.09)	0.06 (0.03)	0.03 (0.03)	1.29 (0)	>25
		2Bl	7	0.31 (0.18)	0.58 (0.09)	0.31 (0.08)	0.11 (0.03)	0.01 (0.01)	1.41 (0.1)	>25
		2BC	6	0.33 (0.21)	0.69 (0.06)	0.27 (0.07)	0.04 (0)	0.01 (0)	1.81 (0.5)	>25

Table 4: Normalized RMSE and ME as validation statistics of the model results, ordered per geomorphic position. Mixed positions are locations where the model follows a different geomorphological setting than was observed in the field. This is due to loss of details with aggregation of the ridge-trough map to the cell size of the input DEM.

		Statistic	Trough	Ridge	Mixed	Total
Gravel	Fraction	ME_n	1.~~683~~583	0.~~118~~187	~~3.829~~4.110	1.~~931~~952
		$RMSE_n$	2.~~381~~446	0.~~223~~255	4.~~181~~489	2.~~443~~561
	Mass	ME_n	0.~~320~~270	0.~~129~~188	1.~~354~~444	0.~~433~~450
		$RMSE_n$	0.~~579~~556	0.~~174~~219	2.~~064~~195	0.~~809~~851
Sand	Fraction	ME_n	-0.~~135~~104	0.~~429~~060	-0.~~341~~369	-0.~~087~~139
		$RMSE_n$	0.~~517~~570	0.~~975~~831	0.~~830~~923	0.~~672~~700
	Mass	ME_n	-0.~~202~~184	-0.~~010~~251	-0.~~555~~606	-0.~~305~~336
		$RMSE_n$	0.~~410~~396	0.~~488~~521	0.~~845~~917	0.~~653~~691
Silt	Fraction	ME_n	~~-~~0.~~043~~002	-0.~~652~~782	-0.~~375~~435	-0.~~228~~239
		$RMSE_n$	0.~~744~~703	1.~~005~~084	0.~~914~~950	0.~~830~~829
	Mass	ME_n	-0.~~060~~025	-0.~~670~~793	-0.~~579~~636	-0.~~299~~313
		$RMSE_n$	0.~~383~~347	0.~~863~~984	~~0.988~~1.049	0.~~690~~723
All sizes	Fraction	ME_n	0	0	0	0
		$RMSE_n$	0.~~638~~673	0.~~320~~343	1.~~033~~134	0.~~679~~727
	Mass	ME_n	0.~~024~~016	0.~~063~~053	0.~~042~~034	0.~~038~~030
		$RMSE_n$	0.~~161~~157	0.~~084~~075	0.~~092~~086	0.~~128~~123
Count	Fraction		17	5	7	29
	Mass		14	5	7	26

11 Figures

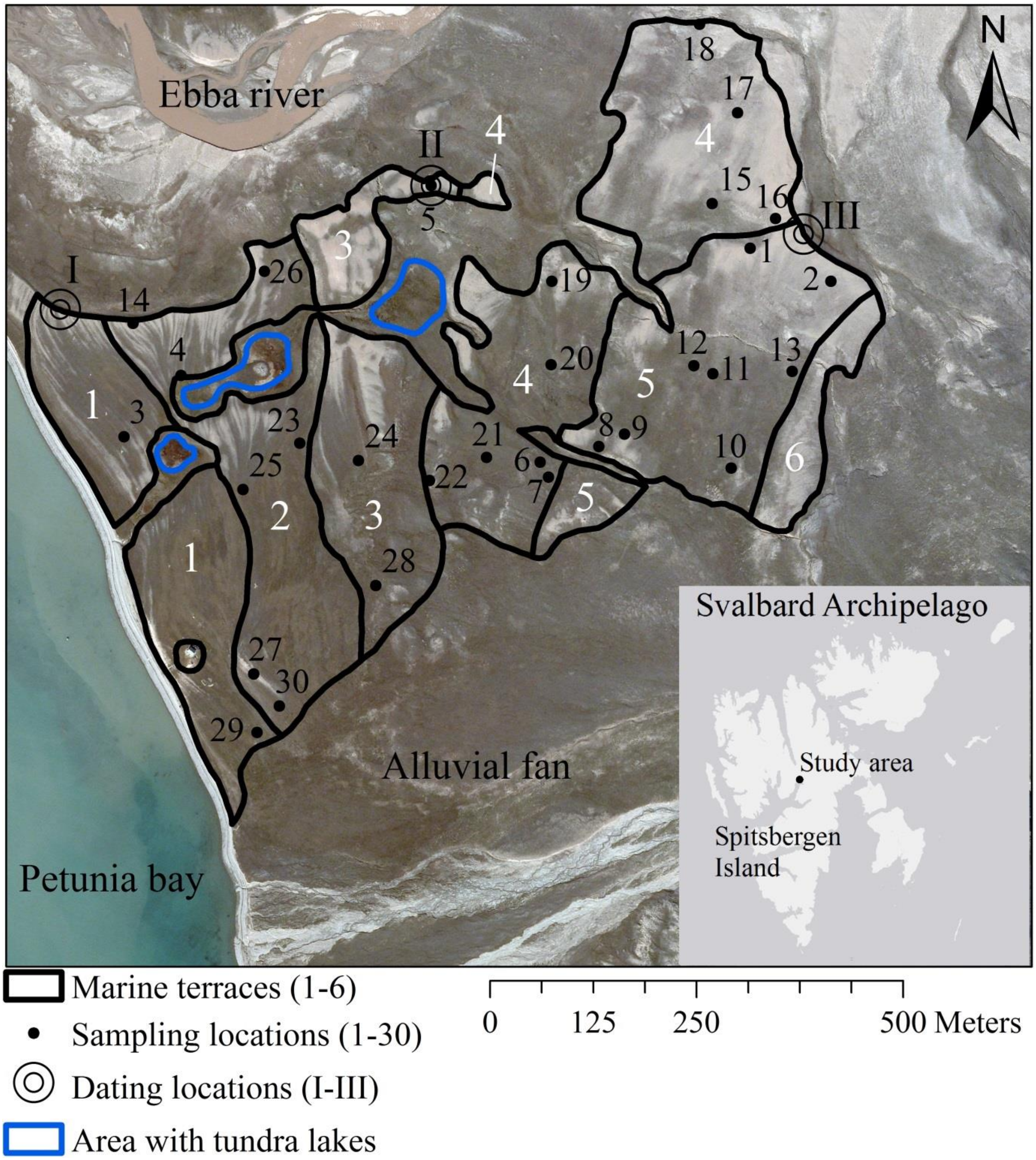
Ebba river
Petunia bay
Alluvial fan
N
I
II
III
1
2
3
4
5
6
7
8
9
10
11
12
13
14
15
16
17
18
19
20
21
22
23
24
25
26
27
28
29
30
Svalbard Archipelago
Study area
Spitsbergen Island
Marine terraces (1-6)
Sampling locations (1-30)
Dating locations (I-III)
Area with tundra lakes
0
125
250
500 Meters

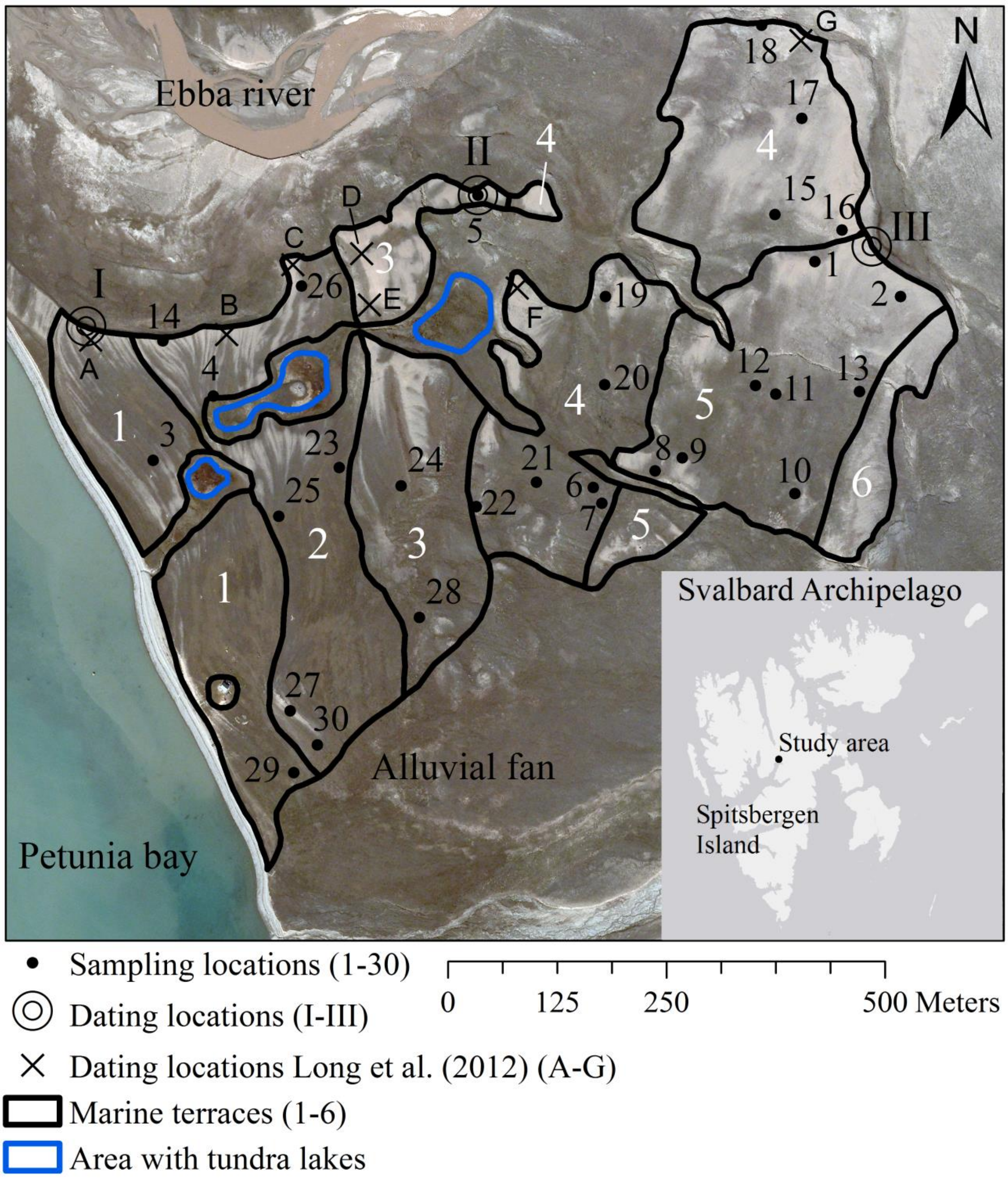

Fig. 1: Aerial photograph (summer 2009) of the study area indicating the 6 terrace levels (in white numerals), 3 OSL-dating locations (in Roman numerals) ~~and~~ 30 sampling locations (in black numerals~~).~~) and the approximate location of the radiocarbon datings done by Long et al. (2012). Their corresponding dates can be found in Fig. 3. Ridges are recognizable as light (un-vegetated) parts of the terraces, troughs are darker (vegetated). Disturbed areas such as erosion rills, permanently wet depressions and tundra lakes were excluded from the study area. The inset shows the location of the study area on the Spitsbergen Island.

1162

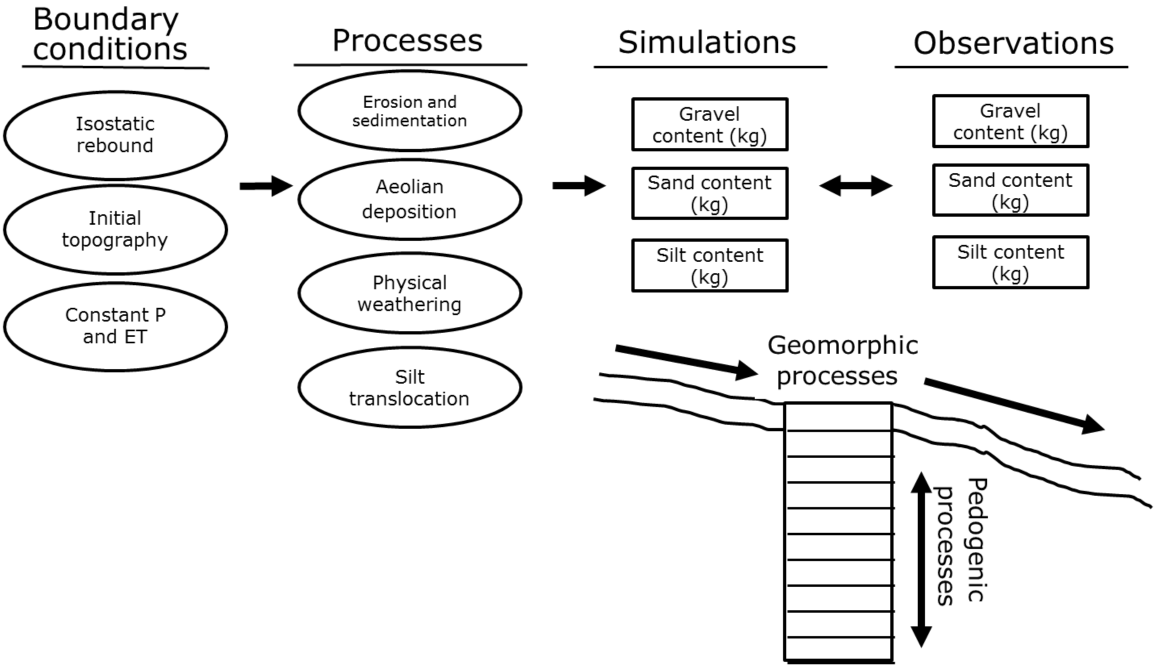

Fig. 2: Conceptual framework of LORICA as used in this study.

1163

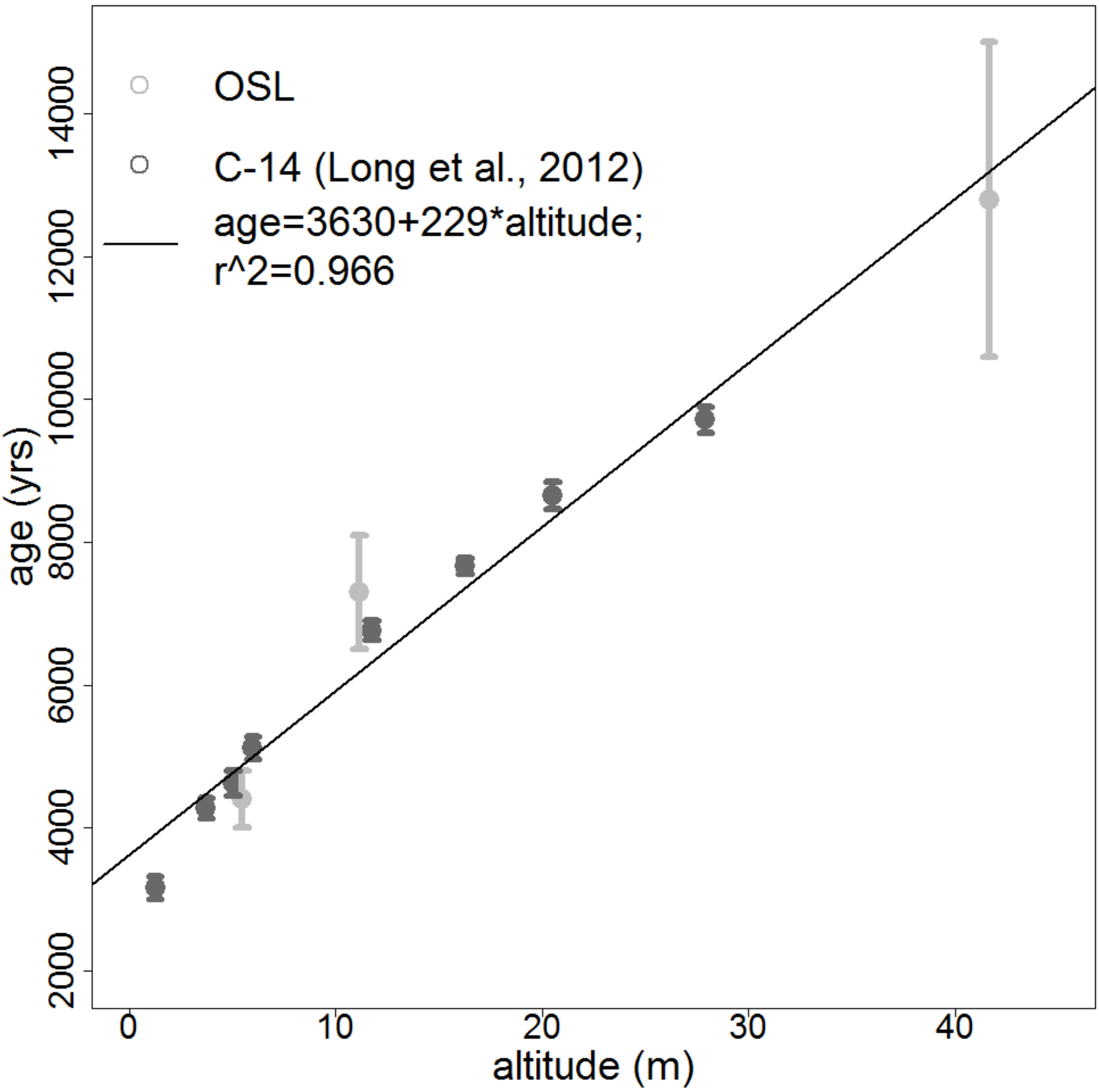
OSL
C-14 (Long et al., 2012)
age=3630+229*altitude;
r^2=0.966
age (yrs)
altitude (m)
2000
4000
6000
8000
10000
12000
14000
0
10
20
30
40

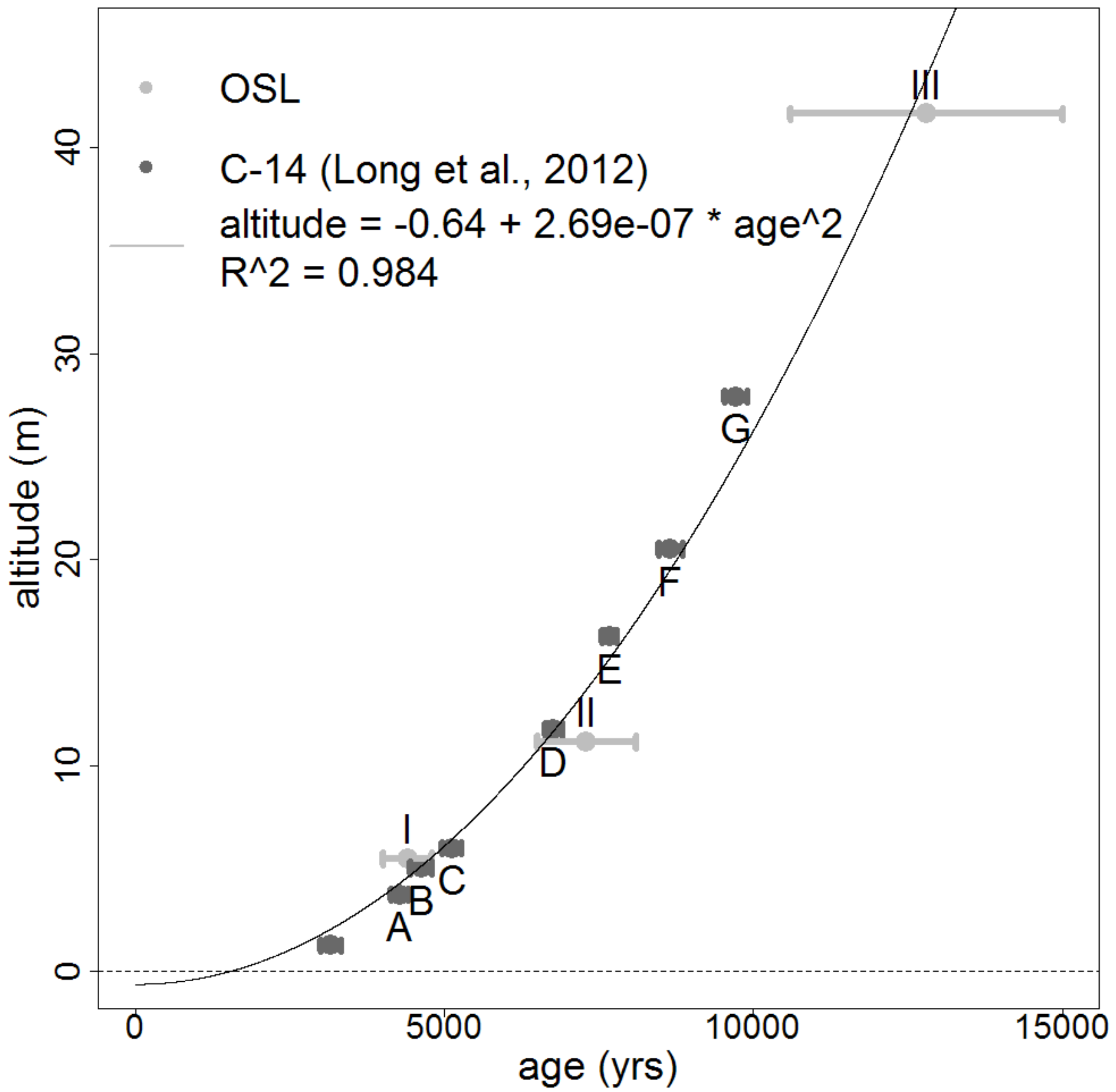

Fig. 3: Elevation and age of OSL dates (this study) and radiocarbon dates (Long et al., 2012). Ages are displayed with a confidence interval of 2σ. The black line shows ~~a~~the linear regression between altitude and squared age of each dating. The symbols A-G and I-III refer to the respective locations in Fig. 1.

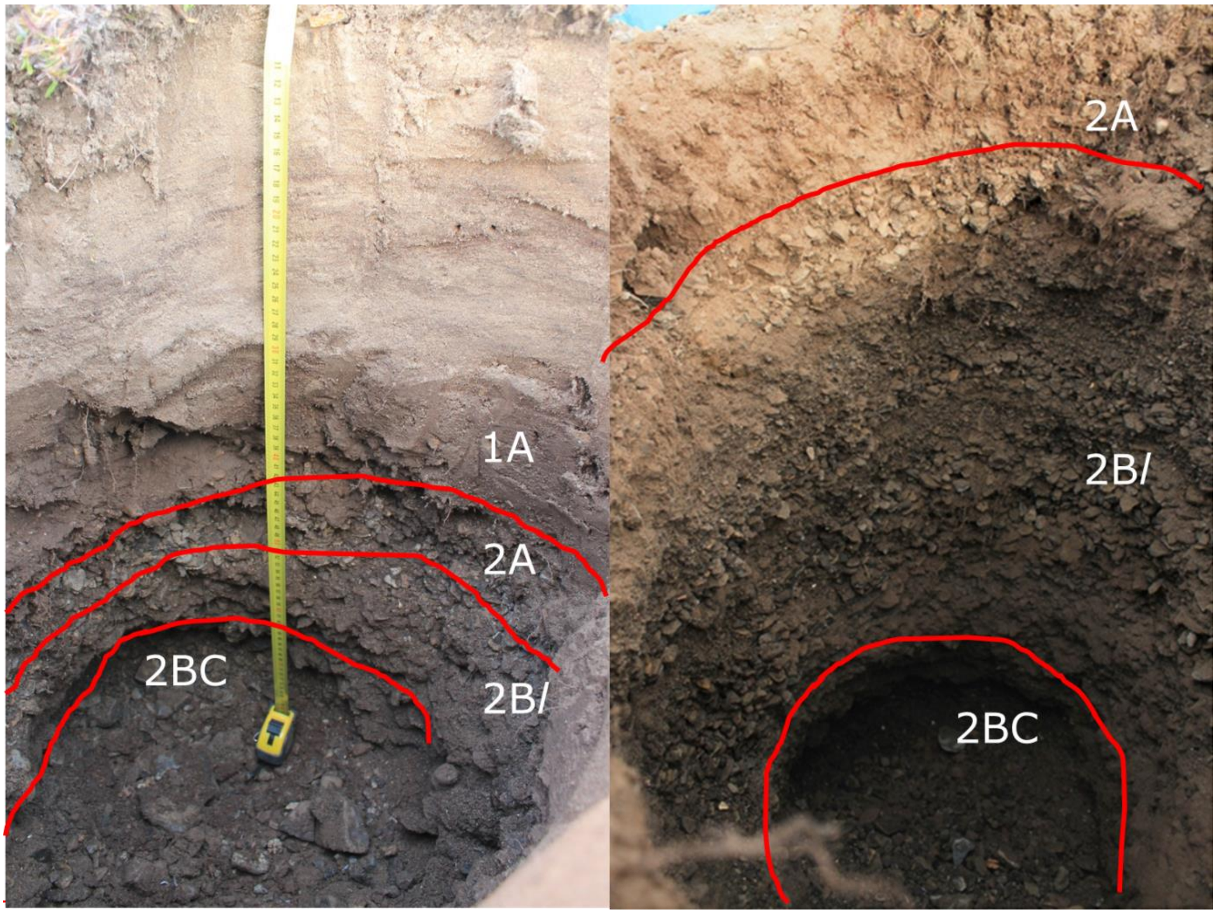
1A
2A
2BC
2B/
2A
2B/
2BC

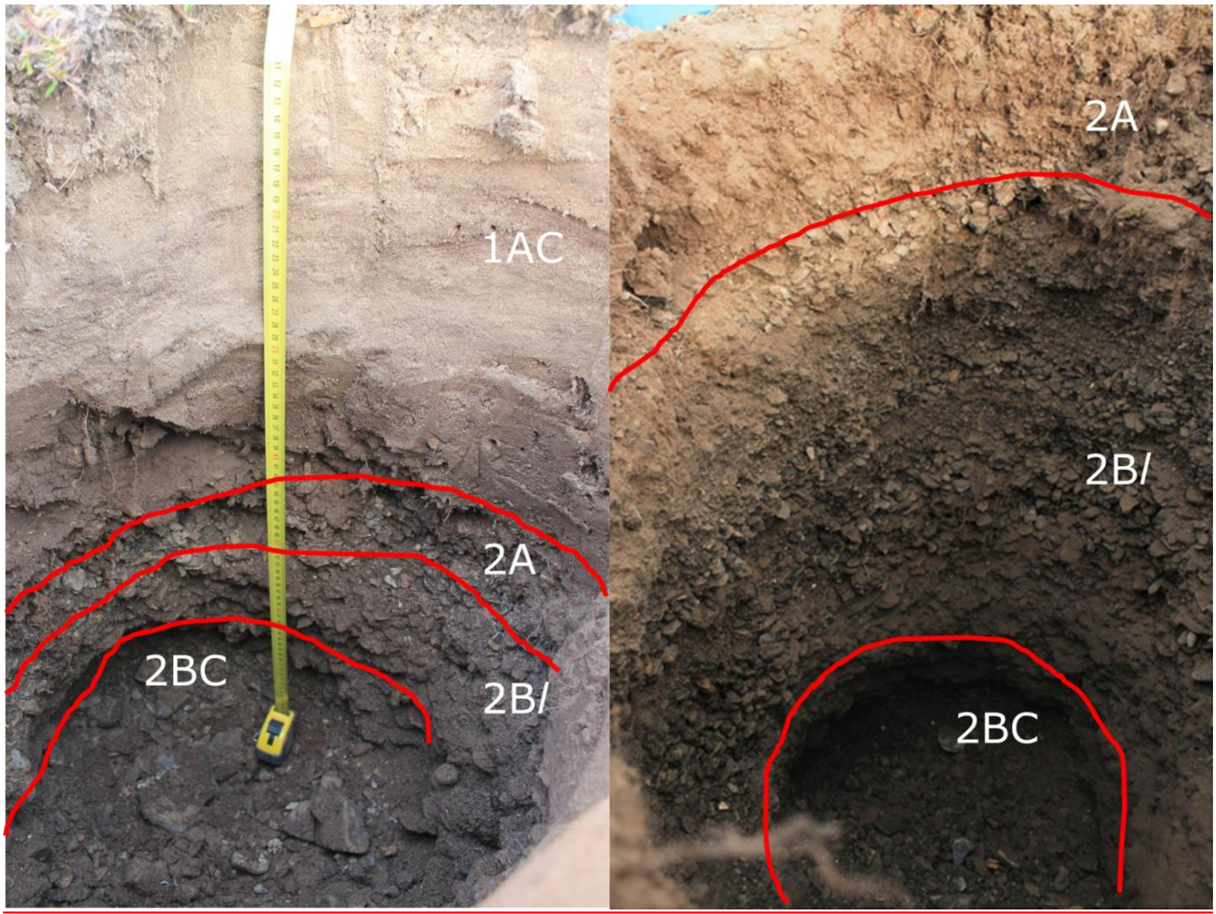

Fig. 4: Examples of a typical soil found on a trough (left) and ridge location (right). The prefixed numbers indicate the parent material: aeolian (1) or marine (2).

1165

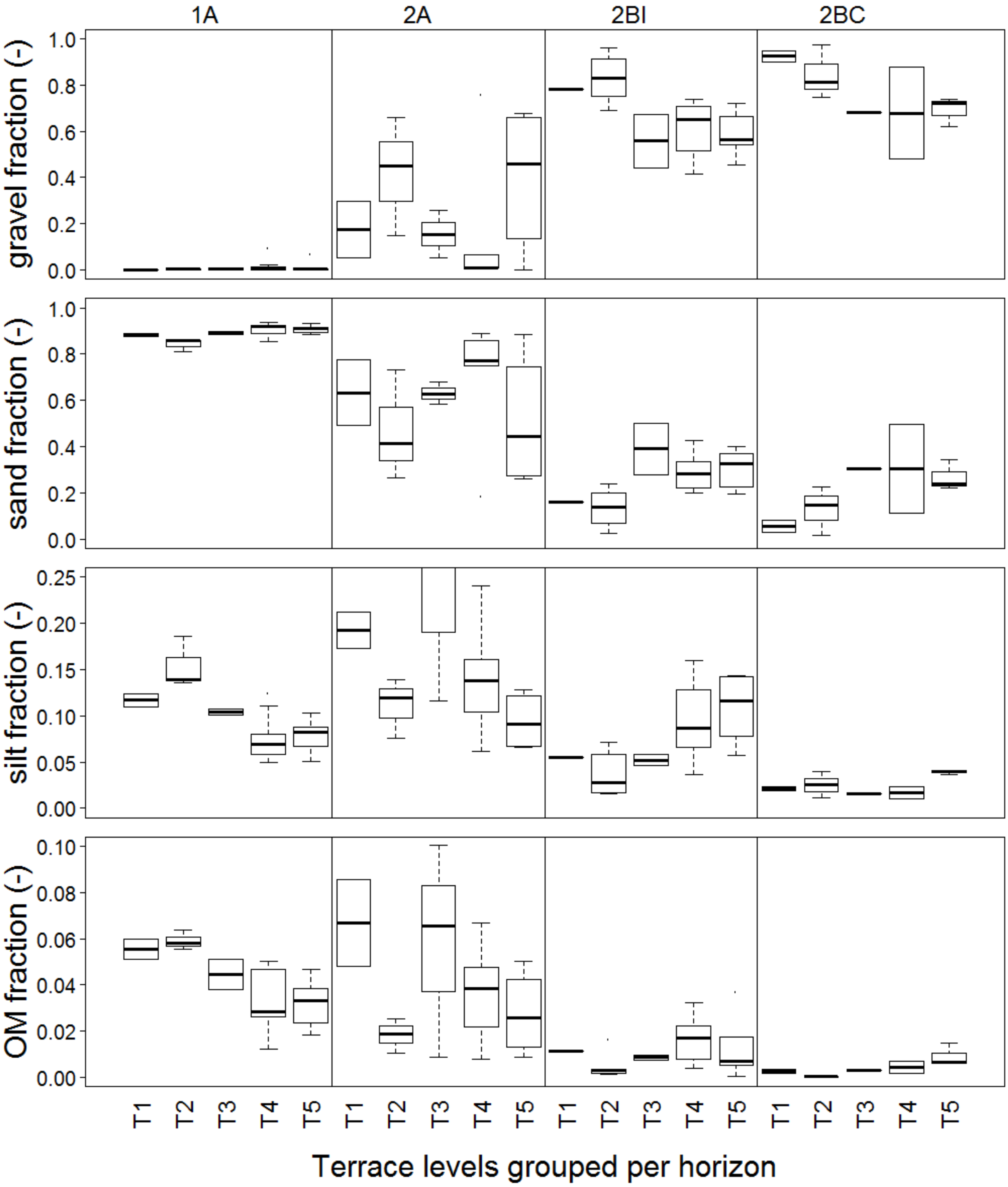

1A
2A
2BI
2BC
gravel fraction (-)
sand fraction (-)
silt fraction (-)
OM fraction (-)
T1
T2
T3
T4
T5
Terrace levels grouped per horizon

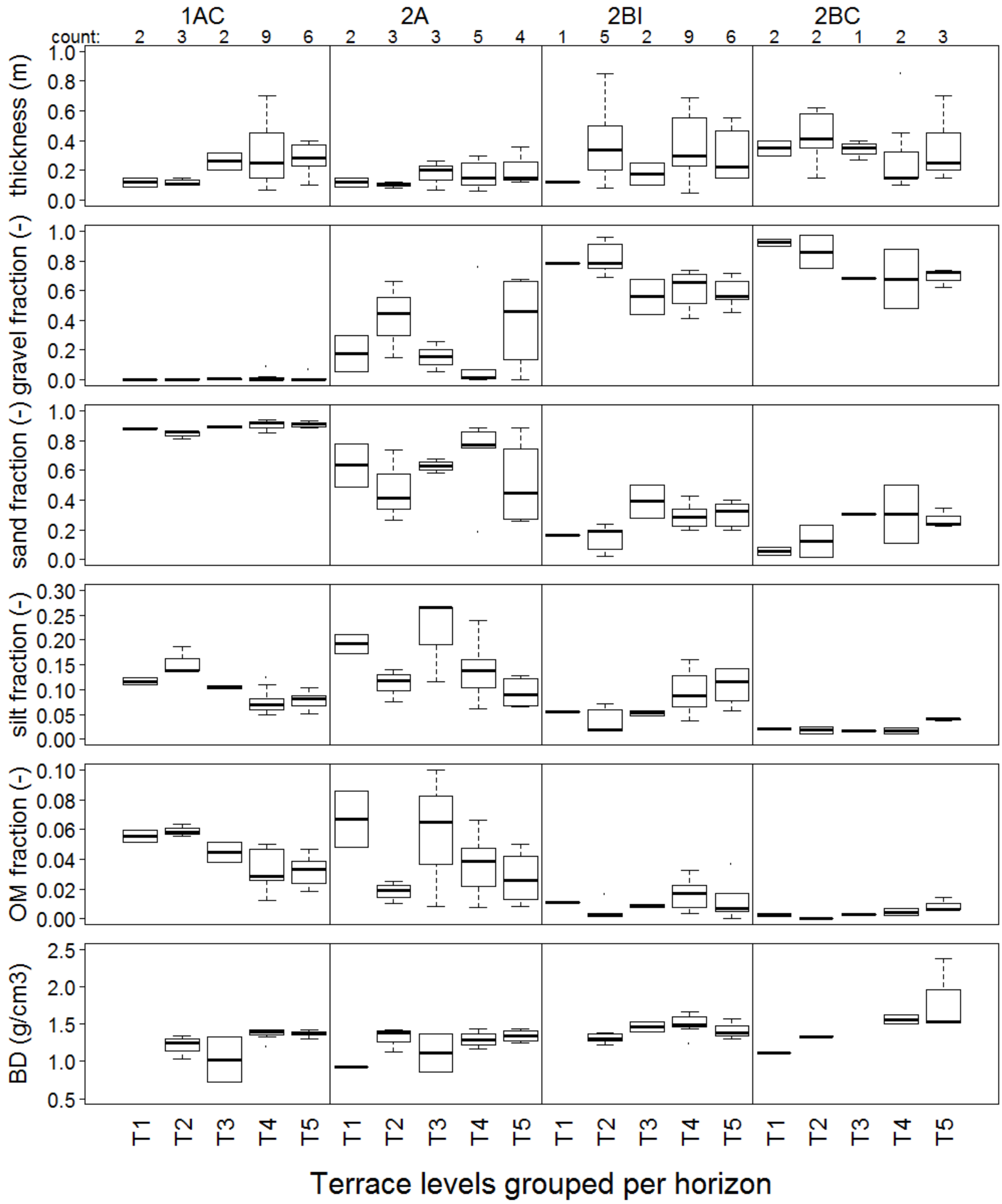

Fig. 5: Boxplots of observed soil properties on different terrace levels, ordered by main soil horizon. Counts indicate the occurrence of the displayed properties. Number of values can differ per soil property due to measurement errors.

1166

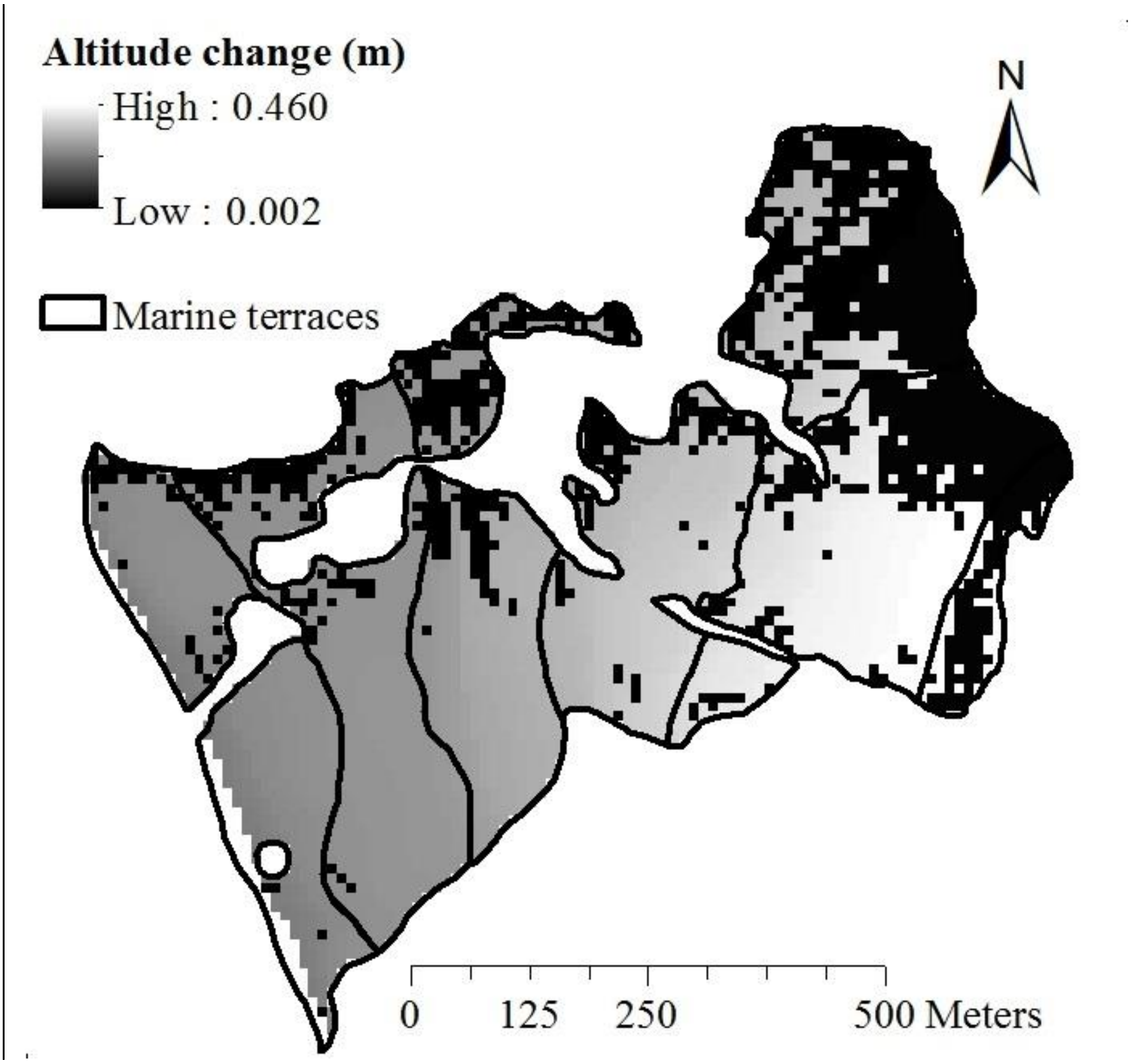
Altitude change (m)
High : 0.460
Low : 0.002
Marine terraces
N
0
125
250
500 Meters

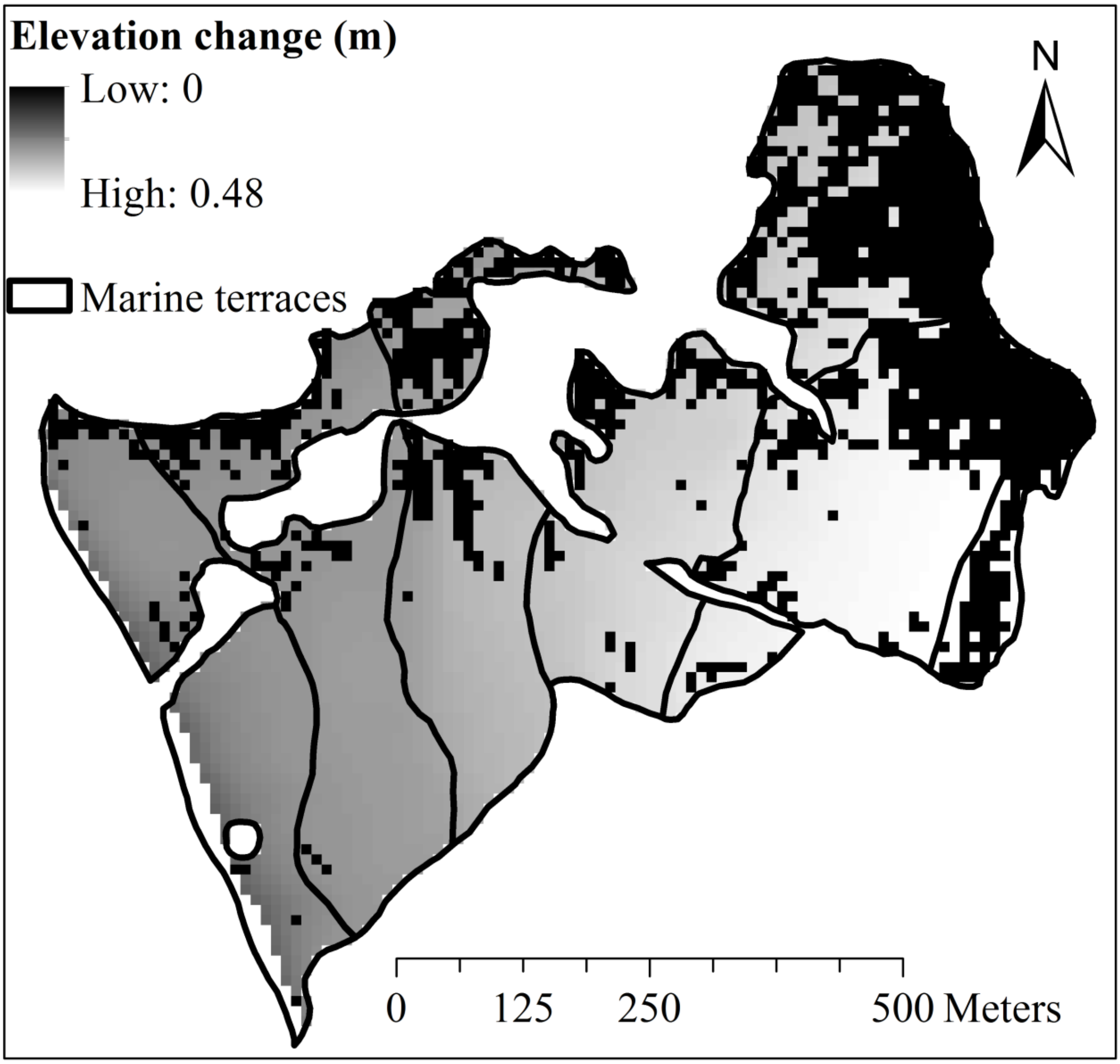

Fig. 6: Simulated altitude change in the study area. A clear difference is visible between ridge positions (black grid cells) and trough positions (grey scales), due to absence of aeolian deposition on ridge positions.

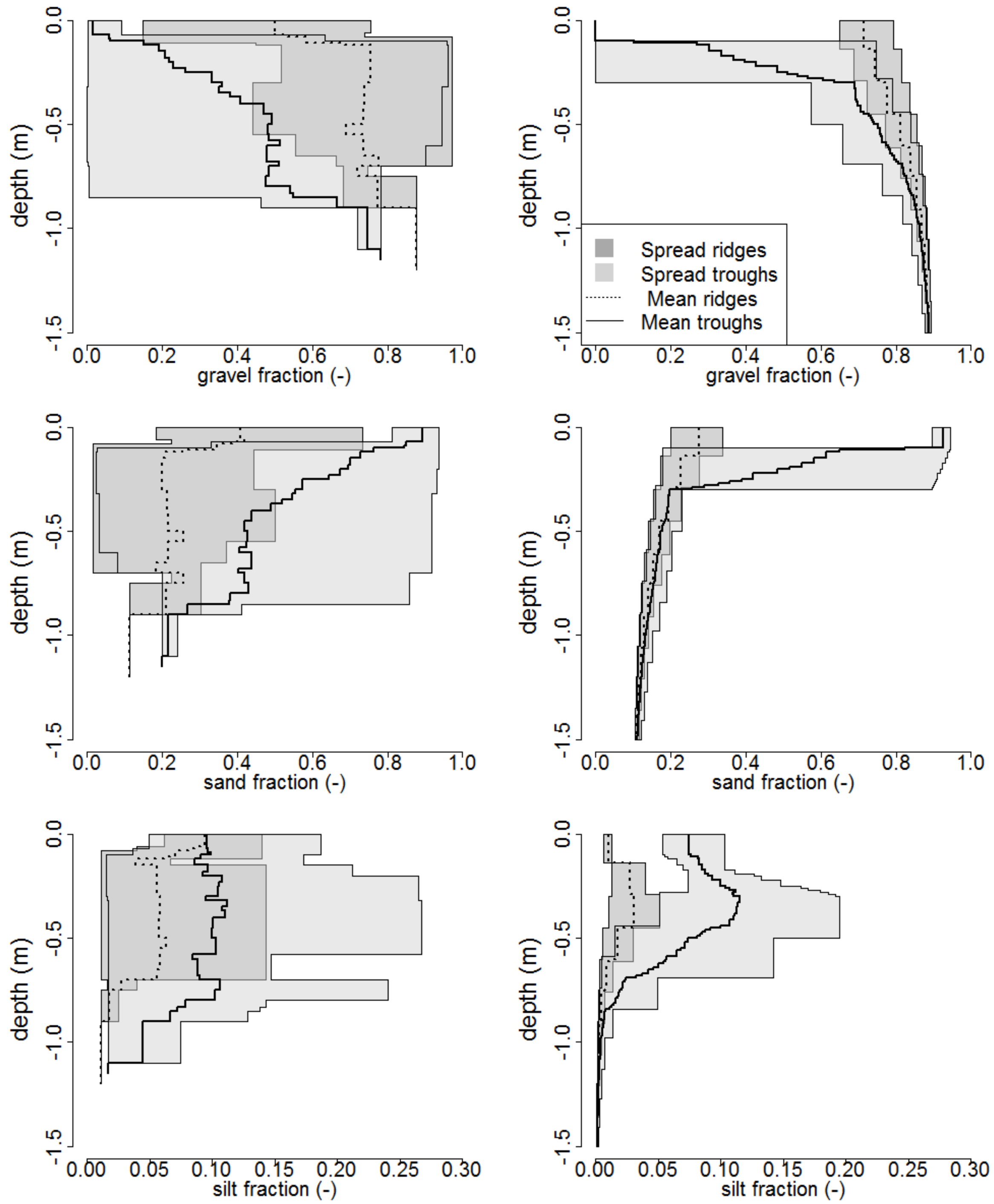
depth (m)
gravel fraction (-)
sand fraction (-)
silt fraction (-)
Spread ridges
Spread troughs
Mean ridges
Mean troughs

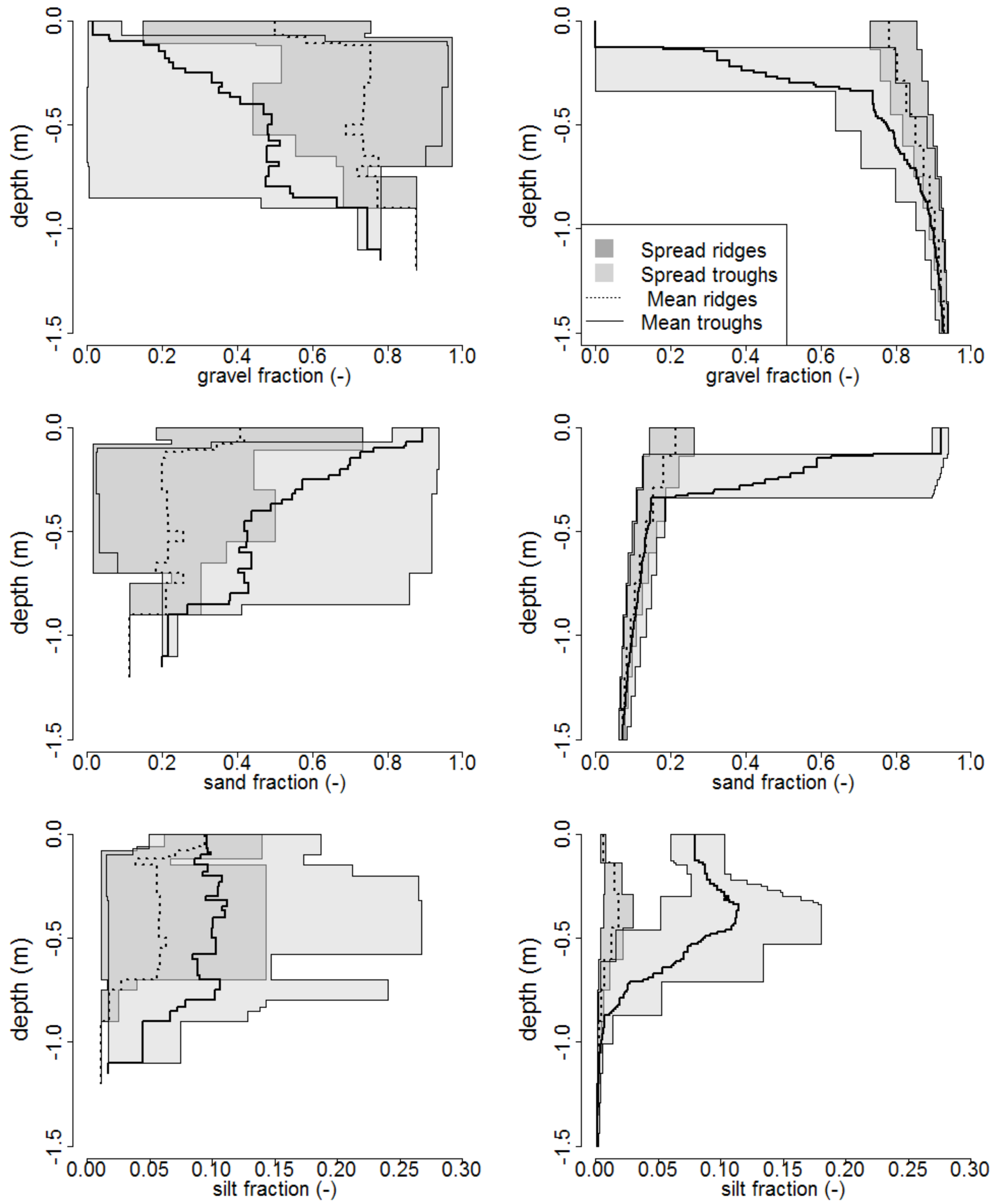

Fig. 7: Total variation and mean of particle fractions in observed and modelled profile curves, divided over morphological setting. For every cm along the soil profile depth, the minimum, maximum and mean mass fraction of the various grain sizes for all profiles in the considered morphological setting are displayed.

1169

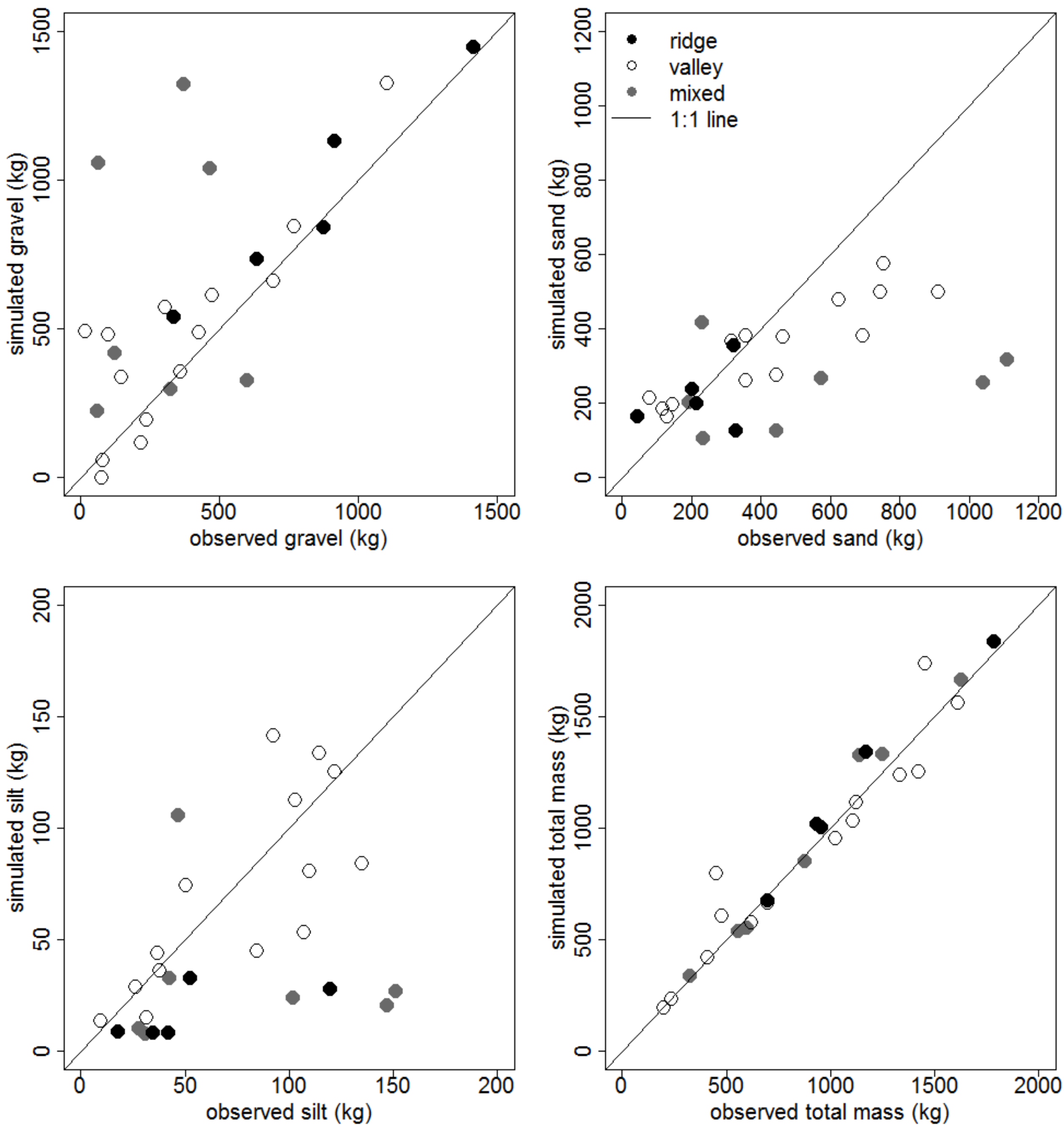

simulated gravel (kg)
observed gravel (kg)
simulated sand (kg)
observed sand (kg)
ridge
valley
mixed
1:1 line
simulated silt (kg)
observed silt (kg)
simulated total mass (kg)
observed total mass (kg)

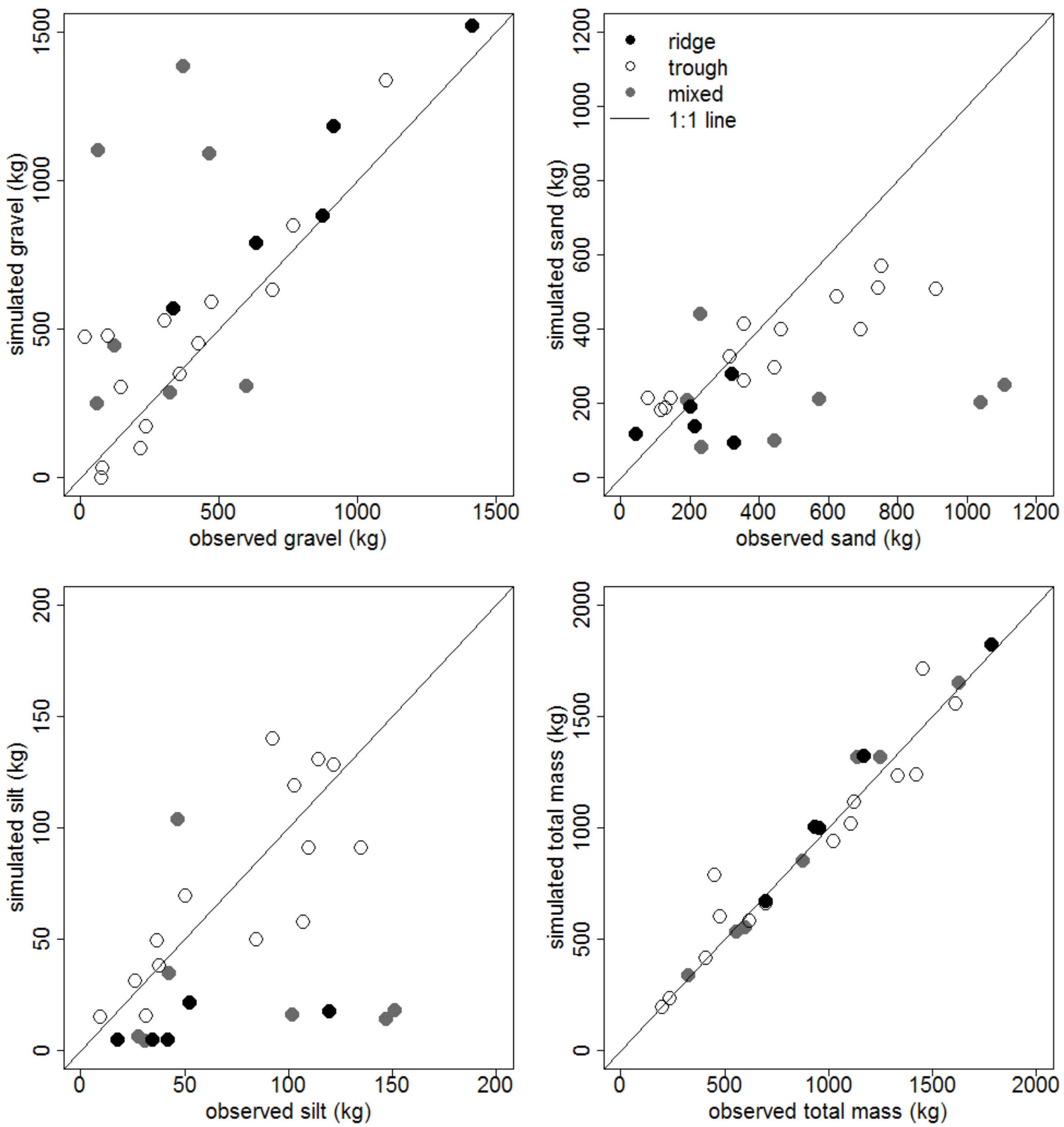

Fig. 8: Scatterplots of simulated versus observed mass in kg over the total observed depth, for different particle sizes and morphological positions. The black line indicates the 1:1 line, which indicates a perfect match between model and field results.

1170